Technical Report

Number 965

UNIVERSITY OF CAMBRIDGE

Computer Laboratory

Improving commercial LiFi network feasibility through rotation invariance, motion prediction, and bandwidth aggregation at the physical layer

Daniel M. Fisher, Jon A. Crowcroft

November 2021

Abstract

In recent years, the number of devices per household has exponentially increased. Additionally, Internet traffic surged during the 2020-2021 calendar years due to the COVID-19 pandemic. Both of these occurrences have served as reminders that the spectrum available for radio frequency (RF) based networking is running thin, as internet service providers had to find creative ways to serve this growth of data demand. Introduced in 2011 by Dr. Harald Haas, Light Fidelity, or LiFi, offers a suitable supplement to ameliorate this challenge as well as offer faster data rates to consumers. However, due to the line-of-sight nature of data transmission required by LiFi, path blockage to the photodetector and natural light obstruction have proven to be significant challenges in commercially implementing the computer network. Hybrid networks have been proposed, serving as a middle ground where the networking load is balanced between LiFi and WiFi depending on which is available. However, many challenges exist with this concept, in particular with optimizing the logic so it is worthwhile.

The goal of this thesis is to further develop this field and push LiFi closer to being commercially practical for the next generation of computer networks. Three lines of effort are pursued to do so. First, the path blockage problem is mitigated through a novel rotationally invariant photodetector configuration that allows for significantly better sensor visibility than previous solutions. Additionally, horizontal handovers from one LiFi hub to another, as a user moves through a space, is improved via leveraging probabilistic machine learning (ML) and other motion tracking algorithms to more accurately predict human movement and identify "hot spots." Lastly, a novel bandwidth aggregation scheme at the physical layer is proposed and preliminarily evaluated through a simulation to significantly improve data rates when both LiFi and

WiFi are available.

Acknowledgements

I certainly couldn't have gotten through this degree and this thesis requirement on my own and would like to take this opportunity to thanks some key individuals that had a significant influence on me.

Dr. Daryl Hartley, my former physics-mechanics professor at the US Naval Academy, has been a great mentor to me for many years. He provided excellent guidance to help me through the physics in the "Rotationally Invariant PD/IR Emitter" chapter of this thesis and pushed me through some challenging sticking points.

Jonah Herzog-Arbeitman was a great help in getting me started on the rotationally invariant sensor portion of this thesis. He is a brilliant physics graduate student at Cambridge and he offered technical advise and pointed me in the right direction early on to get me on the right track to having the baseline knowledge necessary to make progress in this area.

Isaac Sebenius and Adrian Markelov are both close personal friends of mine and not only offered support through the taught portion of this degree, but also kept me inspired and helped me think creatively through problems I faced through some of the challenging technical portions of this dissertation.

I would like to thank Maggie Dods as well for her help with editing for grammar and clarity. Maggie is a brilliant Rhodes Scholar studying at Oxford University and has been a great friend and sounding board during this process.

My parents have both been very supportive and motivational through the challenges of this degree and specifically this dissertation. They have expressed great interest in my work and their excitement in my project has kept me motivated throughout the process.

Contents

List of Figures

List of Tables

List of Acronyms

LiFi   Light Fidelity

WiFi   Wireless Fidelity

RF   Radio Frequency

RL   Reinforcement Learning

ASK   Amplitude Shift Keying

FSK   Frequency Shift Keying

CSK   Color Shift Keying

IM   Intensity Modulation

MM   Metameric Modulation

OFDMA   Orthogonal Frequency Division Multiplexing Access

TDMA   Time Division Multiple Access

SDMA   Space-Division Multiple Access

LOS   Line-Of-Sight

AP   Access Point

WAP   WiFi Access Point

LAP   LiFi Access Point

CU   Central Unit

HHO   Horizontal Handover

VHO   Vertical Handover

RWP   Random Waypoint

BWAPL   Bandwidth Aggregation at the Physical Layer

ORWP   Orientation-Based Random Waypoint

IR   Infrared

PD   Photodetector

List of Acronyms

SMM	Straight Motion Model
UE	User Equipment
IPS	Indoor Positioning System
RI	Rotationally Invariant
DC	Direct Current
BER	Bit Error Rate
TTRE	Time To Return To Equilibrium
RSSI	Received Signal Strength Indicator
QOS	Quality of Service
QAM	Quadrature Amplitude Modulation
PSK	Phase Shift Keying
BWA	Bandwidth Aggregation
TCP/IP	Transmission Control Protocol/Internet Protocol
NRZ	Non-Return to Zero
SNR	Signal-to-Noise Ratio
DL	Deep Learning
CNN	Convolutional Neural Network
MLP	Multi-Layer Perceptron
RNN	Recurrent Neural Networks
FOV	Field of View

1 | Introduction

A piano is a simple acoustic instrument. Most modern pianos have 88 keys, 52 white and 36 black. When a key is pressed, a small felt-covered hammer hits a string encased in the piano, each key producing different tones, the frequencies of which range from 27.5 Hz to 4.19 kHz [47]. Acoustic sensors detect the frequency of sound waves and if one pressed C2 (65.41 Hz) then C4 (261.63 Hz) [72], the two could be distinguished. Additionally, it can be established that C2 and C4 represent a binary 0 and 1, respectively. With this setup, one could theoretically send data and establish a network connection, simply by alternating between pressing C2 and C4. This theoretical piano-based network can be expanded by including more keys so C1 represents 00, C2 is 01, C3 is 10, and C4 is 11. Naturally, this can grow to include more keys and therefore send more bits at a time. So, when a pianist plays a beautiful melody at a concert, they theoretically could also be sending covert messages to communicate with someone who knows the encoding scheme. In fact, any phenomenon that can vary in its nature and can be sensed may be used to represent bits and subsequently send data.

To stream a YouTube video, for example, data must be sent much faster than a few bits at a time, and this is part of why piano networks are not practical, among many other downsides. The concept outlined, however, is analogous to how a Frequency-Shift Keying (FSK) encoding scheme works. This thesis focuses on furthering the development of a light-based computer network that uses Amplitude-Shift Keying (ASK), which is analogous to pressing the keys on a piano with different forces, and Color Shift Keying (CSK), which is similar to playing the same note with different instruments.

Due to the COVID-19 pandemic, there has been a significant increase in reliance on technology as society adjusted to a "work-from-home" environment. Compared to pre-lockdown, internet services have seen usage spike from 40% up to 100% [28]. While companies were able to handle the surge, this served as a reminder of the challenges that lie ahead with RF-based computer networks, specifically that of serving increasingly more devices with higher demands in the Information Age. According to a study done by [38] of thousands of participants, the average number of connected devices per UK household has risen from 7.94 to 9.16 in 2018 and 2020, respectively. Additionally, this exponentially increasing trend is expected to continue with the projected number of devices per consumer increasing to 15 by 2030 [32].

While advances integrated into 5G-technology are tailored to handle increased demand due to the rise of IoT devices, the nature of RF-based networking is inherently limited by the spectrum available and eventually it likely won't be able to compensate. As a result, there has been increased interest in the potential of visible light communication (VLC) based computer networks, as visible light offers nearly 400 THz of unused bandwidth while RF-based networks have around 1,000 times less spectrum available (closer to 300 GHz) and are highly regulated by the Federal Communications Commission (FCC). All of this led to the conceptualization and introduction of LiFi to society in 2011 by Dr. Harald Haas [30]. LiFi has shown great potential, but still faces significant challenges before becoming commercially feasible, this thesis strives to solve some of these problems.

1.1 LiFi Background

Philosophically, LiFi is analogous to WiFi, except it uses light instead of radio frequencies. A reasonable comparison would be that Ethernet is to fiber optics as WiFi is to LiFi. However, from a technical standpoint, LiFi works somewhat differently from WiFi and a promising area of research that this thesis builds upon is hybrid LiFi/WiFi networks. In this section, LiFi will be explained, as well as a hybrid network configuration.

While the IEEE is working on establishing a global standard for VLC called 802.11bb

[12], many different configurations and modulation schemes are possible. The contributions of this thesis except for chapter 5 are independent of the design decisions made regarding modulation scheme and multiuser service, so an example of a typical LiFi system will be explained in this section for general context.

As previously mentioned, any phenomenon that can vary in nature can represent bits. For LiFi downlink, there are a few common modulation schemes including intensity modulation (IM), color shift keying (CSK), and metameric modulation (MM). For each of these, the goal is to maintain constant perceived color and modulate the light at a rate fast enough such that the human eye cannot detect any change. IM simply alternates the brightness or intensity of white light. CSK alternates the intensity of several different colors of light formed into one beam that, to the human eye, is perceived as white [46]. Lastly, MM extends CSK, using a similar technique but including optimizations that allow it to be more energy efficient and maintain less noticeable color/brightness changes in ambient light [15]. For LiFi uplink, either RF or infrared (IR) is common. RF-based uplink applies similar modulation schemes to existing WiFi technology, whereas IR uplink typically uses pulse amplitude modulation with single carrier frequency domain equalisation (PAM-SCFDE) [21, 48].

Naturally, to send and receive these modulations, devices capable of transmitting and sensing the different forms of signal are required. LEDs are used to transmit visual light, and CSK/MM often use a combination of red, green, and blue LEDs. IR emitters are used for uplink. To receive transmissions, photodetectors (PD) and IR sensors are used for LEDs and IR emitters, respectively. For example, say a person is on a couch in their home and wants to watch a YouTube video. Their uplink request is sent via an IR emitter on their mobile phone, which is received by an IR sensor on the ceiling. The request is processed and the video is transmitted via MM emitted from a ceiling light overhead, which is received by a PD on the user's device. For many users simultaneously connected to the same LiFi hub, time division multiple access (TDMA) and space-division multiple access (SDMA) are possible, although orthogonal frequency division multiplexing access (OFDMA) is the most common

multiplexing technique [53, 69]. Figure 1.1 shows a visual of an example LiFi system in an office.

Figure 1.1: Example of LiFi System in an Office Setting [42].

As of 2017, LiFi's expected data rate was 100 Gbps [35], 100 times faster than 4G/LTE Advanced (1 Gbps) and 10 times faster than what is expected of 5G technology (10 Gbps) [59]. However, LiFi requires line-of-sight (LOS) transmission, while RF-based systems do not. This is an advantage from a security perspective, but it also creates a significant challenge that has been the focus of a great deal of research in the field. Specifically, path loss due to blockage of the PD or IR sensor becomes a problem due to direct blockage (e.g user covers the sensor) and/or increased incidence angle (e.g user rotates the device). Natural light interference due to the sun is also a concern [2]. As a result, hybrid LiFi/WiFi networks were developed and continue to be a promising area of research in making LiFi commercially feasible.

Since visible light and RF do not interfere with one another given that they use entirely different parts of the electromagnetic spectrum, load balancing between LiFi/WiFi is a natural solution to the path loss problem. A great deal of research [3, 61, 63, 65, 66, 67, 69, 71] has been conducted into finding ways to transition between LiFi/WiFi depending on which is available and optimized for best quality of service (QoS). Figure 1.2 shows an example configuration of a hybrid LiFi/WiFi network.
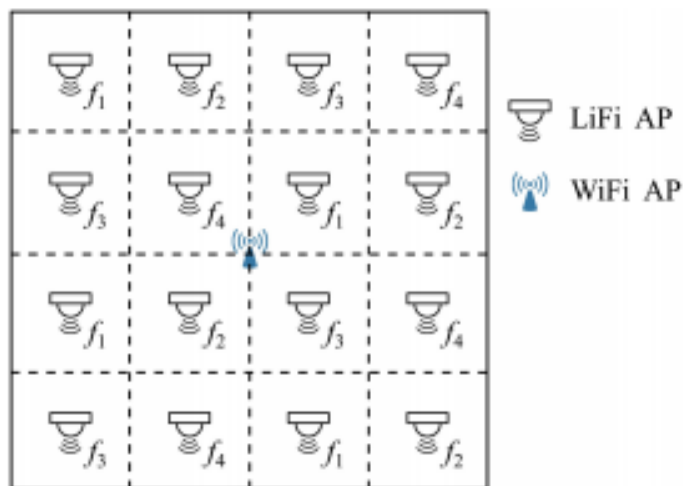
Figure 1.2: Example of LiFi/WiFi Hyrbid Network [66].

In figure 1.2, the room is assumed to be square with 16 lights in a 4x4 configuration. Each light is considered a LiFi access point (LAP) and there is one WiFi access point (WAP) in the middle of the room. Additionally, this configuration would contain a central unit (CU) controlling the system as a whole and allowing the programmer to implement the logic necessary to switch between LiFi/WiFi access points (AP) in a sophisticated and optimized manner. A handover between a LAP to another LAP (e.g the user is walking) is called a horizontal handover (HHO) and a switch between a LAP to a WAP (e.g the PD is no longer visible due to path loss) is termed a vertical handover (VHO). To simulate user mobility, the random waypoint (RWP) model is commonly used. RWP assumes that waypoints are randomly distributed throughout a space and users move in a straight line from waypoint to waypoint at constant speed, varying speed, or varying speed with pausing [67]. Furthermore, in [27] the orientation-based random waypoint (ORWP) model was discussed, which models rotation angle as a Gaussian random process, accounting for the angle of incidence of light to the PD due to device rotations.

1.2 Thesis Focus and Contribution

LiFi offers great potential but currently has limitations, specifically path loss due to blockage and rotations, as well as natural light obstruction. Hybrid networks offer a middle ground that accounts for these vulnerabilities, but still faces challenges before it can be commercially implemented. Many papers have addressed these issues as

explained in chapter 2, and the academic community has made great progress in refining and improving this form of network.

This thesis pursues three primary efforts to further develop this field and push LiFi closer to being commercially practical for next generation Internet connection. The first two focuses address the issue of path loss. Firstly, VHOs are far more detrimental to system performance than HHOs, so it is advantageous to minimize their occurrences. This can be done through increasing sensor visibility through a novel rotationally invariant (RI) PD/IR emitter configuration. Additionally, as explained in section 1.1, the RWP and ORWP are standards for simulating user movement and are the basis upon which a great deal of research was built. However, human movement is more predictable than random motion, as people have certain tendencies and "hot spots" exist within a room. It has been proven that performing efficient HHOs is key to system performance, and these can be done more effectively through predicting user movement rather than relying on the RWP/ORWP or straight motion model (SMM). With ML, human tendencies can be learned within each respective space, tracked by the CU, and leveraged to perform better HHOs. Other tracking algorithms that identify "hot spots" could also prove effective at accurately modeling human movement. Lastly, hybrid networks have primarily been used in the past to conduct load balancing between LiFi and WiFi. This means only one form of network is used at a time, which, while using less energy, does not leverage the full capabilities of the system. A great deal of research has been conducted into performing bandwidth aggregation (BWA) between WiFi and broadband cellular networks, and the same concept can be applied to hybrid networks to take advantage of cases where both LiFi and WiFi are available. Furthermore, to the author's knowledge, there has been no previous research into BWA at the physical layer (BWAPL). With increased focus on synchronization between LiFi and WiFi signals, this can be achieved and significant improvements in data rate are possible due to increasing the number of modulation levels.

The remainder of the thesis is organized as follows. Chapter 2 covers related works and previous research. Chapter 3 includes the methodology of the first idea presented

in this thesis on a RI PD/IR emitter configuration, Chapter 4 focuses on using ML and other tracking algorithms to better predict user movement for handovers, and chapter 5 discuses LiFi/WiFi BWAPL. Chapter 6 concludes the thesis and offers suggestions and opportunities for future research, although future works will be discussed throughout the thesis as well.

2 | Related Works

The invention of hybrid LiFi/WiFi networks are an essential development to this research, as all contributions of this thesis build upon its structure. [63] wrote one of the early papers on hybrid networks, describing a load balanced system between LiFi/WiFi that selects one or the other based on blockage of the PD. However, this paper did not account for user movement, and later research by [69] established a basis for realistic indoor hybrid networks accounting for both rotation and translation. [67] explored static load balancing, assigning users up front to either LiFi, WiFi, or both based on their visibility. Additionally, [8] studied strictly using LiFi for downlink and WiFi for uplink. Lastly, [21] focused on using IR for uplink, which, as described in the introduction, is the standard assumed network that will be discussed later in this thesis.

The contributions of this thesis are threefold: (1) improve PD/IR emitter visibility through implementing a RI configuration (2) improve handovers by better predicting user movement using ML and other motion prediction algorithms (3) increase data rates in situations where both LiFi and WiFi are available through BWAPL. While, based on the author's extensive literature search, these ideas are novel, many related works have inspired them or work in conjunction. The next three paragraphs cover related works for each respective idea in the order listed above.

[26, 40, 53, 58] studied the impact of device orientation on network performance. These papers will be used as benchmarks on path loss due to sensor visibility when discussing the improvements of a RI sensor. Two omnidirectional PD configurations were presented in [20, 44] which involve placing sensors on multiple faces of the device so that it will maintain visibility regardless of rotations. However, [26, 53, 63]

proved that greater angles of incidence lead to worse network performance. While this idea solves the issue of having no sensor visibility in scenarios where the device is facing down, for example, it still will experience path loss due to angles where light is between two sensors and neither sensor has enough visibility to yield a high quality data rate. These papers served as inspiration for developing a novel configuration where the PD was free to rotate about 3 axes so it maximizes light visibility in all cases possible.

In [65], a handover skipping technique is discussed to optimize HHOs. Based on reference signal received power from a device that is received and the rate of change of the signal, the AP the user is moving towards is predicted. To predict future user motion, the SMM is assumed, which is a naive assumption and motion can be predicted in a more nuanced manner using ML. In this thesis, the goal is to generalize this concept, as human movement is often erratic. When walking from the kitchen to the couch, for example, it is unlikely that the individual maintains a constant velocity, and naturally when they sit on the couch, their velocity will stop. By using probabilistic ML or similar movement prediction algorithms, it is possible to learn tendencies in a room rather than predicting without considering prior knowledge. In [66], VHOs and HHOs are explored in a mobility-aware model where users are statically assigned up front to strictly LiFi or WiFi, or a hybrid of the two to load balance. [7] used deep learning (DL) to predict a device's current position based on received signal from IR uplink. While [7] was able to achieve excellent accuracy (18 cm) that challenges current state-of-the-art indoor positioning systems (IPS), to improve the hybrid network as a whole it is essential to predict where a user is going rather than where they are, although knowing one's current position can be used as input to a predictor system on user trajectory. [49] used LiFi to develop an IPS to very accurately determine user equipment (UE) position as well. A few papers have used ML to perform optimal load balancing. [61] used a form of reinforcement learning (RL) called multi-armed bandit to do AP assignment based on an objective of maximizing overall throughput for users being serviced. Similarly, [3] used RL for AP assignment with a reward function focused on average network throughput, user

satisfaction, fairness and outage performance. While these papers achieved reasonable success, it is theorized that different room configurations lead to people moving throughout those rooms in predictable manners and the formation of "hot spots." So, if a ML algorithm was trained on user position over time, it is believed that a more successful hybrid network can be achieved based on performing sophisticated AP assignment. Neural Networks and other non-ML related algorithms are also believed to be good candidates for tracking human movement and will be discussed.

While BWA remains largely unexplored in a hybrid LiFi/WiFi network, many papers in the past have studied it regarding broadband cellular networks and WiFi, when both are available. In [33, 43, 50, 70], BWA at the transport layer was considered involving 3G and WiFi. After 4G became widespread, [5] did the same for 4G and WiFi. [25] researched multipath TCP for smart mobile devices on software defined networks. BWA has been explored at the network/IP layer as well, typically requiring the use of proxy servers to aggregate signals [1, 23, 24, 29]. Additionally, at the data link layer, link aggregation solutions have been developed, typically in the context of web or mail servers [16, 17, 18, 19]. The closest research to this idea was by [8, 55, 71], who studied multipath TCP for LiFi and WiFi. When both are available, BWA at the transport layer is performed, and if LiFi signal drops, the system falls back on WiFi. To the author's knowledge, no prior research has been done into BWAPL for any kind of network including hybrid LiFi/WiFi networks. Furthermore, it is theorized that this could significantly increase modulation options, increasing the number of bits that can be sent at a time and subsequently the data rate as well.

3 | Rotationally Invariant PD/IR Emitter

3.1 Concept Formation

As established in section 1.1, a typical LiFi system uses MM with visible light downlink to a device and IR uplink. For the purposes of this thesis, a common indoor scenario will be considered where LAP's are the overhead ceiling lights (LEDs) in a room. Naturally, these lights are statically placed and their beam will be focused orthogonally to the floor, but spread at the half-power semiangle which will be discussed in more detail in this chapter. While numerous devices can connect to LiFi, the focus will be on mobile phones, as their orientation is far more dynamic than other devices such as laptops, smart tvs, or smart speakers (e.g Alexa). Due to the small size of mobile phones, society's heavy reliance on them, and their being held in different orientations, cellular devices are believed to be one of the more difficult devices to load balance in a hybrid network. To support the standard indoor scenario described, mobile devices, henceforth referred to as User Equipment (UE), will require an IR emitter and a PD to handle uplink and downlink, respectively. Most papers assumed that UE always faces upwards towards the LAP for simplicity, but in reality this is a bad assumption; to make LiFi more commercially practical, variations in orientation must be considered. In this chapter, it will be demonstrated by reviewing the work of [26, 40, 53, 58] that it is ideal to have maximum visibility between the IR emitter/PD on the UE and the LAP and this can be achieved through a novel RI configuration.

3.2 Detailed System Configuration

In this indoor scenario, it is assumed that LED lights are statically placed on the ceiling and face vertically downward. Additionally, it is assumed that no reflective objects in the room distort the propagation of light and that the LED follows the Lambertian radiation pattern. The LAP and UE positions are given by (x_a, y_a, z_a) and (x_u, y_u, z_u), respectively, and d simply gives the Euclidean distance between AP and UE. Figure 3.1 helps visualize the scenario and shows some important variables that will be discussed.
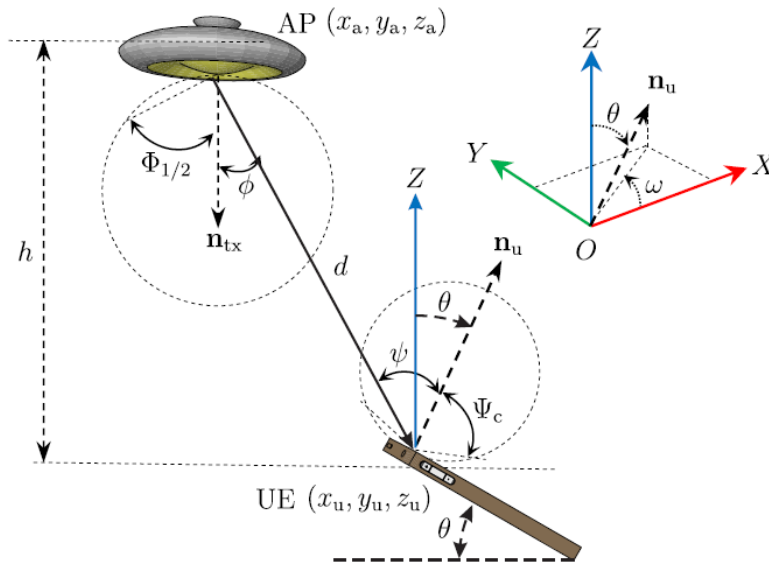
Figure 3.1: Indoor LiFi Configuration [26].

n_{tx} and n_u give the normal vectors to the LED and UE, respectively, and will be used as references for other key variables. ϕ is the angle between n_{tx} and (x_u, y_u, z_u), known as the incidence angle. Furthermore, ψ represents the radiance angle with respect to the normal vector n_u. $\Phi_{1/2}$ essentially describes the propagation coverage of a LAP and is known as the semiangle at half power, which is the angle at which the luminous intensity is half the axial intensity. In figure 3.1, θ gives the pitch of the UE, although rotation angles are more clearly shown in figure 3.2. With these terms in mind, the direct current (DC) gain between the AP and UE is expressed by the following equation as derived in [26]:

$$H = \frac{(m+1)A_{PD}g_f h^m cos(\psi)}{2\pi d^{m+2}} rect(\frac{\psi}{\psi_c}) \tag{1}$$

where m, also known as the Lambertian order, is equal to $\frac{-1}{log2(cos(\Phi_{1/2}))}$, A_{PD} is the area of the PD, g_f is the gain of the optical concentrator based on the refractive index (S) and the UE field of view (FOV) (Φ_c), and h is the vertical distance between the AP and UE [26].

It is essential to establish a basis for UE rotations as well, as that most often leads to path loss. Assuming that the coordinate system is set up as shown in figure 3.2 (a), the y-axis is in the direction of the length of the phone, the x is the direction of the width, and the z is orthogonal to the device's screen plane.
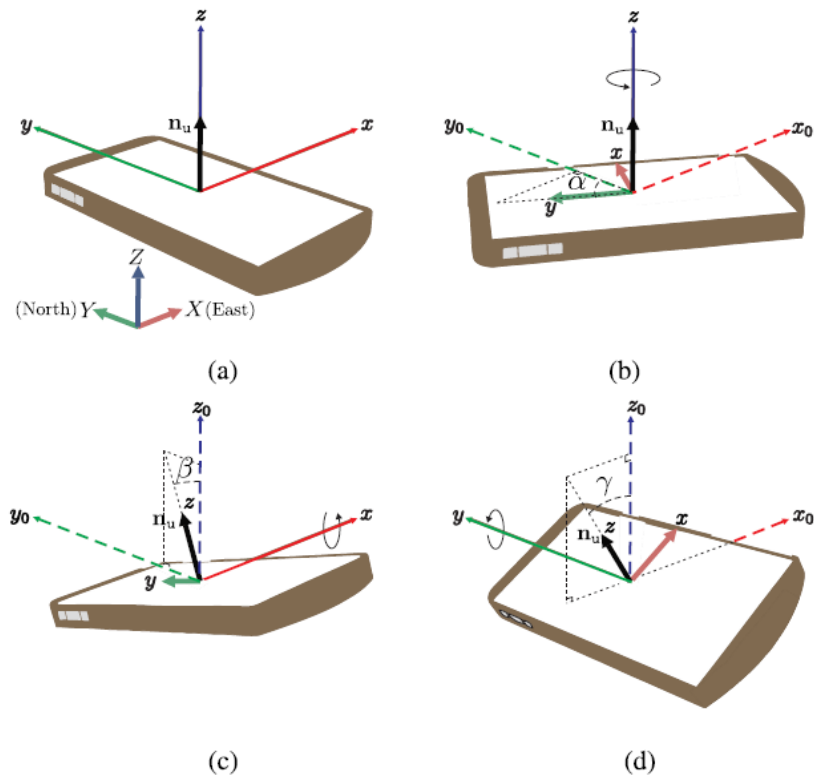
Figure 3.2: UE Rotations (a) Standard Unrotated Position (b) Rotation about the z-axis of Angle α (yaw) (c) Rotation about the x-axis of Angle β (pitch) (d) Rotation about the y-axis of Angle γ (roll) [26].

As shown in figure 3.2, rotations can occur about three axes. A rotation about x is called pitch and denoted as β or in spherical coordinates as θ. Yaw is a rotation about z and is denoted as α. Lastly, roll is a rotation about y and expressed as γ. To calculate n'_u, or the normal vector to the UE after a rotation, a matrix multiplication is done between R, the rotation matrix ($R = R_\alpha R_\beta R_\gamma$), and n_u [26]. ω represents the angle between the absolute positive x-axis and the direction of the phone. This variable is extended to better represent the direction the user is facing as Ω, which equals $\omega + \pi$.

It was shown in [26, 51, 57] that θ follows a Laplace distribution where the mean user angle is 41° sitting and 30° standing. Additionally, it was determined that Ω follows a uniform distribution.

3.3   Ideal UE Orientation

In [26], it was proven that having UE optimally tilted towards the AP has a significant impact on channel gain and bit error rate (BER). To prove this, a scenario was set up where four users were placed in different locations in a room with one AP that was central. Each user had a fixed Ω of 45° and FOV of $\psi_c = 90°$. Based on changing the pitch θ of UE, DC channel gain described by equation (1) changes based on the user's location given by (x_u, y_u, z_u). Figure 3.3 shows both channel gain based on different user locations as θ varies, as well as the experimental configuration.
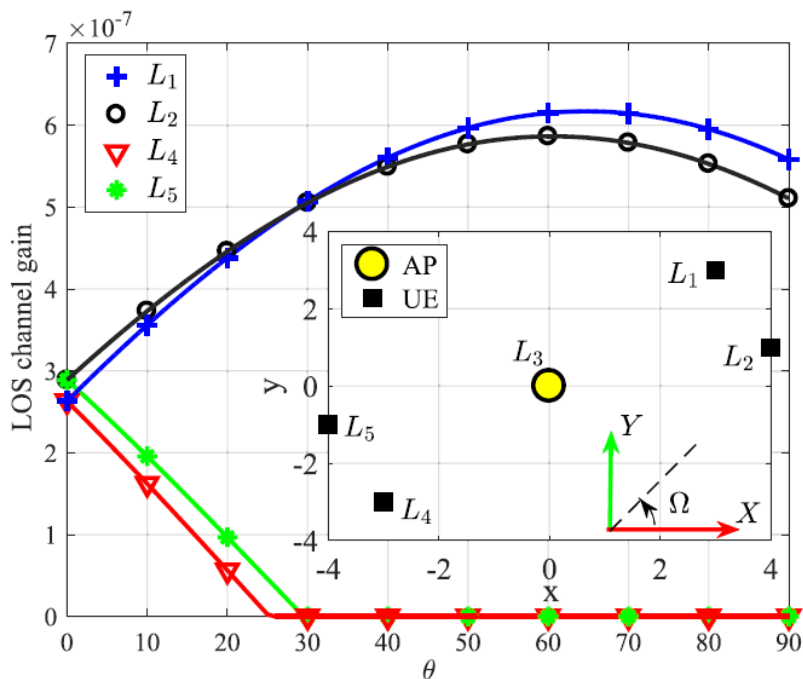
Figure 3.3: Experimental Configuration Given by Interior Figure and LOS Channel Gain Based on Variations in θ Shown in Outer Plot [26].

Considering figure 3.3, it makes sense that channel gain drops off for L_4 and L_5 as θ increases because all users are facing $\Omega = 45$. So, L_1 and L_2 essentially have their backs to the light and as they tilt their phones towards their body, naturally the PD more directly faces the AP at L_3. The opposite is true for the other two users who are facing the AP and tilt their phones away from it, towards their body. On the other

hand, if L_4 and L_5 tilted their devices to negative θ angles, channel gain would increase.

Furthermore, if θ and all other variables are held constant and Ω is varied, figure 3.4 shows the change in channel gain for all values from $0°$-$360°$. θ is set to $41°$ (dashed line), as that is the mean angle for sitting [51, 57], and θ_{th}, which is the threshold yaw, or maximum angle that will always have non-zero gain regardless of variations in Ω. ψ_c is held at $90°$.
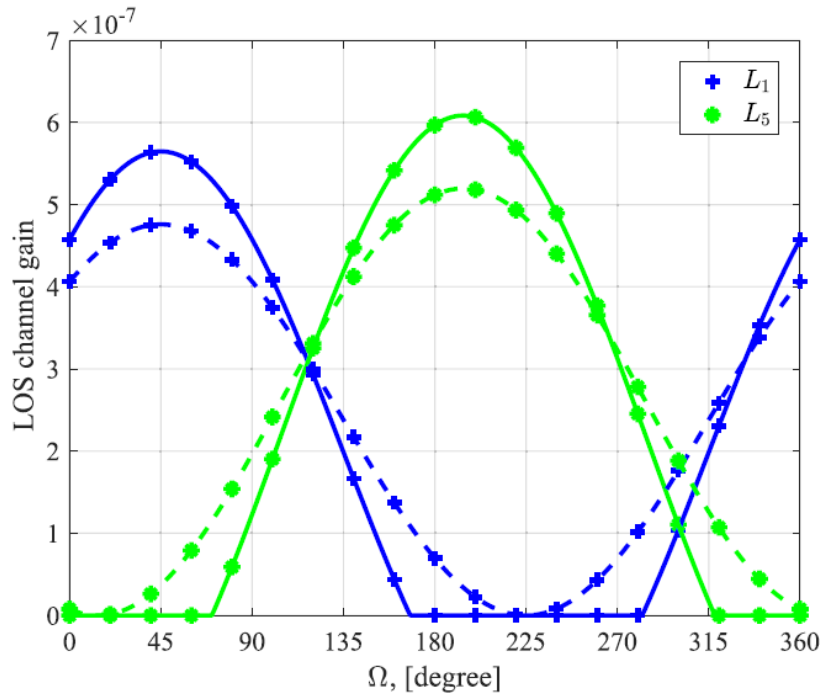
Figure 3.4: Variation in Channel Gain Due to Changes in Ω; Dashed Line Shows $\theta = 41°$, Solid Line Shows $\theta = \theta_{th}$ [26].

It is clear from figure 3.4 that channel gain is heavily influenced by changes in Ω, as well as θ. For $\theta = 41°$ when channel gain goes to 0 between $\sim 170°$ and $\sim 275°$ in L_1, for example, this situation would be one where hybrid networks become useful. In a load balanced configuration such as the one explained in [69], when the gain drops below a certain value to the point where BER is too high and data rates are too low, the UE would be switched from LiFi to WiFi. Similarly, when channel blockage rises above acceptable levels again, they could be switched back to LiFi, if the system configuration allows for it.

Adding multiple LAP's solves many issues with channel gain dropping to 0 at certain angles. Consider the inner figure of figure 3.3 showing the experimental

configuration. The user at L_4 can be visualized as tilting their device towards their body and, as shown by the red line in figure 3.3, this quickly leads to channel gain dropping off. However, say the setup shown is just the first quadrant of a room with origin at the current value of (-4,-4) and each other quadrant was identical to the displayed one. This would mean there are now four LAP's and as the angle of θ increases and channel gain drops, a HHO could be performed with another LAP behind the user in accordance with [65] (although [65] used reference signal received power to indicate when handovers were necessary), keeping them connected via LiFi. Of course this will still be an issue with the outer edges of the room, and that challenge is addressed by the novel RI sensor configuration presented in section 3.4.

There are two essential behaviors that are clear from figure 3.3 and 3.4 that both inspired the idea presented in section 3.4 and prove its validity. First, the fact that each variation in angle had some maximum shows that there is an ideal PD angle for each configuration. Secondly, the existence of θ_{th} is crucial, as it demonstrates that there is some angle such that channel gain will never be 0, assuming constant roll. These two phenomena should be kept in mind as the novel RI sensor configuration is discussed in the next section.

3.4   Proposed Rotationally Invariant Configuration

In section 3.3, it was proven that there is an ideal angle for the PD for each UE configuration. A UE configuration is defined as the combination of all variables (roll, pitch, yaw, 3D position, Ω) describing exactly where the device is. At this ideal angle, the device receives best QoS and in the load balancing scheme, LiFi will be more available, which is advantageous since it offers more bandwidth, yielding better data rates and allowing more devices to share a network. Given an ideal angle for each UE configuration exists and previous works have shown that the UE configuration can be determined very accurately [11, 26, 49, 61], the problem is now clear: how can it be ensured that the PD and IR emitter have maximum visibility and are positioned in these ideal angles?

As mentioned in chapter 2, previous works have looked into this. Managing handover skipping [65, 66] for HHOs was a crucial development and it is very useful to handover to more visible LAPs if they are available in cases like where L_4 in figure 3.3 tilts their device towards their body. Rather than staying connected to the AP at L_3, where their gain significantly dropped, it would be ideal to switch to an AP behind the user, if it exists. However, HHOs are more expensive (concerning latency) than staying connected to the same AP [65, 66]. Furthermore, VHOs are more expensive than HHOs, and [65, 66] proved that minimizing handovers is optimal. So, while the work on handover skipping has been useful, as algorithms were developed to minimize VHOs and optimize HHOs, it still remains advantageous to perform fewer handovers in general, assuming QoS remains high. This technology has already been developed, so the original question then becomes more specific: how can it be ensured that the PD and IR emitter have maximum visibility and are positioned in these ideal angles, while minimizing the number of handovers required?

Previous approaches found to this problem regarding physical sensor configuration were by [20, 44], where PDs were placed on multiple faces of the device so that signal could be received regardless of device rotations. The problem with this idea is that when the device is rotated partially between faces, neither PD will detect modulations very well. It was proven in [26, 53, 63] that these greater angles of incidence lead to path loss and are less ideal than a particular optimal angle. It also requires more complexity to coordinate received signals from multiple PDs.

Instead, it is proposed that one single PD and IR emitter are used and they are configured on a three gimbal system, thus allowing the system to freely rotate in three dimensions. This configuration, similar to a gyroscope, has three rings, each of which are orthogonal to the other ring planes. On the innermost ring is a disk that has the PD and IR emitter positioned on top, such that it will be parallel to the plane of the LAP. However, rather than relying on the law of conservation of angular momentum, which keeps the disk oriented in this manner like a gyroscope, a counterweight is used. This mechanism allows the disk and subsequently the sensor/emitter to quickly return to its desired position (this will be quantified soon), but without the

additional power requirement and variance in performance (if the rotation axis is ever even slightly offset due to natural human movement) that maintaining a perpetually spinning physical disk does. Furthermore, this configuration ensures that regardless of rotations in the device-except for two very unlikely situations that will be discussed soon-the PD/IR emitter will always be oriented vertically upwards after some delay which will be shown to be insignificant. While the previous section proved that vertically upward orientations are not always optimal such as if one is in position L_4 in figure 3.3, it has been proven in [26] and is trivial to conclude that when a device is rotated from any position, it is ideal to have the sensor facing upwards towards where all APs are rather than away from the APs. In section 3.5 more advanced mechanisms will be discussed that ensure optimal angles at all times and are an area for future research.

The RI system will now be explained in detail and the physics behind its implementation will be quantified. Figure 3.5 shows a visualization of the proposed design on a phone, and figure 3.6 illustrates a close up view of the three gimbal system.
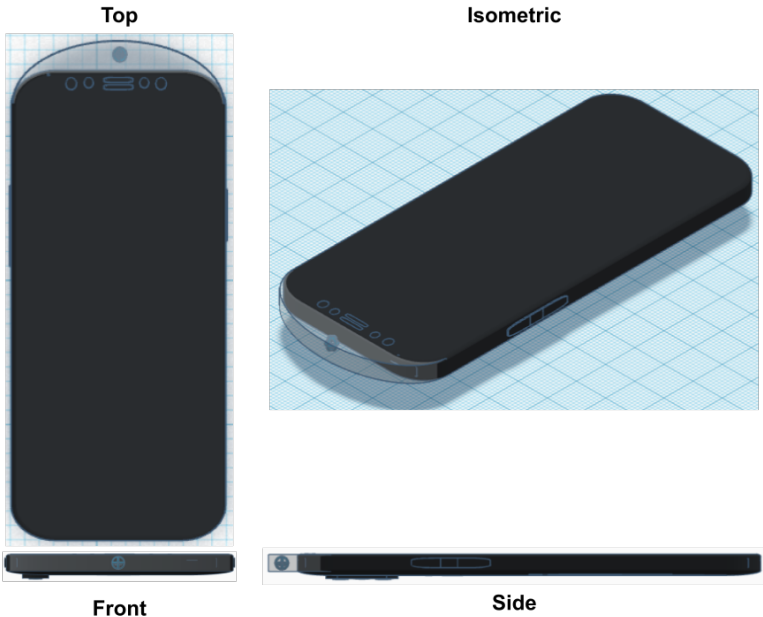

Figure 3.5: RI Sensor Configuration on a Cellular Device.
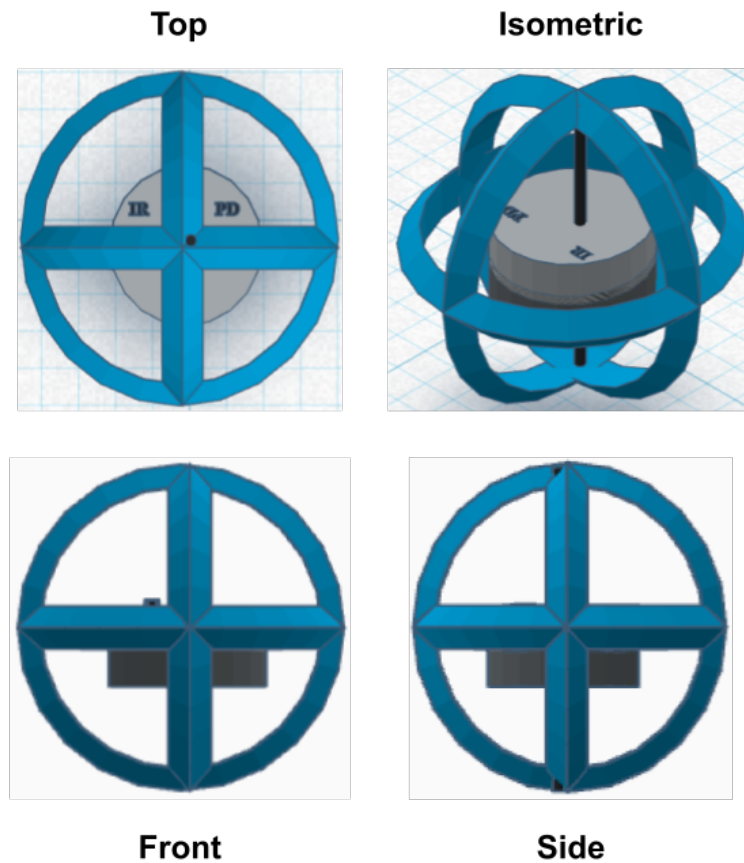
Figure 3.6: Enhanced RI Three Gimbal PD/IR Emitter Configuration.

For the purposes of this chapter, a cellular device will continue to be referred to as UE and will be shown in CAD sketches, although a similar approach could be used for other devices and would have the same physics. Figure 3.5 shows UE with a small, transparent casing extending off the the front of the device encasing a three gimbal system as shown in figure 3.6. Details such as the wiring necessary for the PD/IR emitter and the mounting of the system are omitted for clarity and are left as an engineering problem for future research, should this idea be adapted. They are important to note, however, as they are critical in making the configuration effective and practical. Furthermore, this setup is only one option for mounting the RI system. It is important, though, that the system is mounted in such a way that it is not obstructed by the device. It is necessary to note that the rings surrounding the disk could block the PD/IR emitter; thus, in a practical implementation, they should be thinner than in the CAD sketch in figure 3.6.

As previously mentioned, the system contains three rings, each of which is

orthogonal to the other two rings. Moving towards the center, each successive ring is slightly smaller in diameter (this is not visible in figure 3.6), and they are connected via gimbals. A pole goes through the innermost ring and is connected to the ring at opposite ends of the circle. On this pole are two cylinders stacked on top of one another, the bottom of which has more mass. A PD and IR emitter are mounted on top of the upper cylinder, facing vertically upwards.

This three ring system was chosen, as it allows for rotations about the x-, y-, or z-axis without changing the innermost ring's angle, although this is dependent on the coefficient of static and kinetic friction of the gimbals. Additionally, a heavier cylinder was placed under a lighter cylinder, opposite the sensors, so acceleration due to gravity would always make the configuration seek a position where the heavy cylinder was facing down and the sensors were subsequently facing up. Figure 3.7 describes the effectiveness of this design in relation to the rotation of UE about the y-axis (roll).
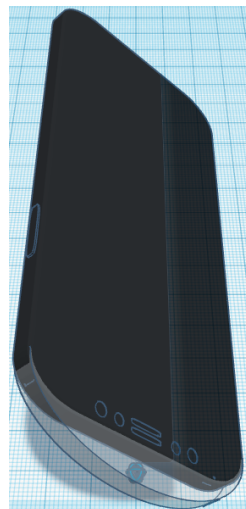
Figure 3.7: Rotation about the y-axis of UE by $\gamma = 45°$.

Several assumptions about this system are important to specify. First, it is assumed that the system begins at rest, meaning there are no oscillations in the RI system and the device begins with 0 velocity. Torque (τ) is then applied by physically rotating the UE as shown in figure 3.7, for example. Rotations about the z-axis (yaw) do not affect PD/IR visibility, as these simply involve spinning the device while keeping it parallel to the ground and LAP, and will not be further discussed. Each inner ring is connected at two points (the gimbals) with the adjacent ring to it and these

connections are assumed to evenly distribute the weight of that ring. Lastly, rotations are assumed to be two dimensional, purely about the x (pitch) or the y (roll). In reality, depending on the system, rotations could be considered decoupled, meaning the rings of the system rotate independent of one another, or coupled (dependent). However, assuming they are coupled goes beyond the scope of this thesis and requires higher order differential equations to describe the motion due to the non-linearity of the relationship, as the torque due to gravity opposing the torque due to friction (due to human rotation) changes over time. As such, the relationship between rings are assumed to be independent of one another, so the time to return to equilibrium (TTRE) with a rotation equals the max of the TTRE for each axis. So, a rotation purely about the x or the y would focus all torque in one direction, as the torque is given by equation 2.

$$\tau = rF * sin(\theta) \tag{2}$$

θ describes the angle between the radius vector and the force vector, so to achieve maximum torque, $sin(\theta)$ must equal 1, which is only the case for pure rotations about an axis. Regardless of the torque applied to the gimbals leading to rotation in the inner cylinder, the key metric is TTRE, as this influences whether or not a VHO takes place and this will be analyzed for all possible angles.

For the purposes of this thesis, the following situation is considered: UE is rotated about the x or the y with some torque τ. Based on the friction in the gimbals, the inner ring with the cylinders rotates to some angle θ, thus offsetting the PD/IR emitter. After coming to rest due to the opposing force of torque due to gravity, the weight of the lower cylinder causes the inner ring to rotate back to a position where the sensors are parallel to the AP plane. The inner ring will oscillate as it returns to this position, which can be arrested through several methods. Then, the system returns to rest with the PD/IR emitter facing vertically upwards again.

In figure 3.7, a torque is applied to the UE, rotating it from rest about the y-axis by $45°$. This scenario can be broken up into three parts from a physics standpoint. The first component of the problem encompasses how far offset the ring and subsequently the

PD/IR will be. This section takes place from the time the system is initially at rest $(\tau = 0)$ until the torque on the system is again 0 when the ring stops rotating at its apex at $45°$. The second part of the problem involves the time the ring takes to return to its starting position from $45°$ due to the force of gravity on the heavier, lower cylinder attached to the inner ring. This takes place from the time the last part of the problem left off until the device returns to facing vertically upwards. However, this return will include oscillations so the final component of the problem requires that the system be arrested in the intended position to stop these oscillations and more quickly return the PD/IR emitter to an upwards-facing configuration.

In a theoretically ideal scenario, the gimbals would be perfectly frictionless, and there would be no offset due to rotations in the UE whatsoever. However, in practicality this is not the case, although modern gimbals have very low coefficients of friction. The offset angle of the innermost ring, which is the primary consideration as this determines the PD/IR visibility through rotations, is based on two opposing torques in this rolling problem: the torque due to friction from the physical rotation of UE and the torque due to gravity opposing this motion. These forces are variant over time, as torque due to friction is strongest initially and decreases as torque due to gravity increases, until the two are equal and net torque is 0. At this point, the ring will be at rest at its apex as shown in figure 3.8.
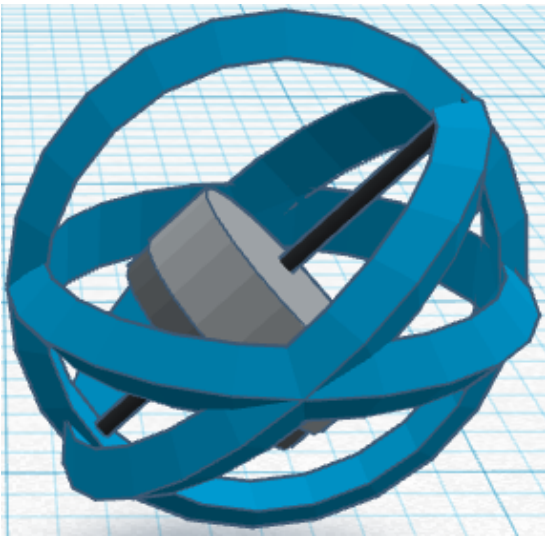

Figure 3.8: Enhanced View of RI System After Rotation about the y-axis of UE by $\gamma = 45°$.

As mentioned, the torques acting on the system vary over time and their derivations

are beyond the scope of this thesis. However, for the purposes of evaluation of the system performance and its impact on VHOs, a very conservative assumption is made that the coefficient of static friction is never overcome and the angle the inner ring rotates to equals the angle that UE was rotated. This is an extremely safe assumption, as modern gimbal technology is far better than this, so it is important to remember that the analysis on part two of this problem hinges on a worst case assumption and in reality the system should significantly outperform these metrics. So, after a roll of $45°$ of the UE, the inner ring is also assumed to be offset by $45°$.

Once the motion of the ring has stopped and the torque is 0, part two of the problem is essentially a pendulum problem. In this case, perfectly frictionless gimbals are not ideal, as frictionlessness leads to greater periods of the pendulum. So, for simplicity and to be conservative, another worst case assumption is made: assuming that the gimbals are perfectly frictionless. It was previously mentioned that the ring would oscillate after the offset in the first part of the problem, only slowing due to friction. This gave rise to the third part of the problem requiring that the ring be arrested in the position where its PD/IR emitter are facing vertically upwards. For this thesis, it is assumed that the arresting mechanism in part three of the problem is effective enough that the TTRE is $\frac{1}{4}$ of the pendulum's period, as any oscillations after arresting will be negligible and not affect PD/IR visibility. Section 3.5 will discuss the many ways that the system can be arrested.

The most important metric in this scenario is TTRE, as it influences whether or not a VHO takes place based on the time that the PD/IR emitter are not visible to the AP. As discussed, part two of the problem is a simple pendulum where the length of the pendulum (L) is defined by the distance from the fixed rotation axis (where the frictionless gimbals are) to the center of mass of the pendulum. In this case, the system can be treated as a point mass and the location of the point can be determined based on the equation for center of mass given by equation 3.

$$y_{cm} = \frac{m_1 y_1 + m_2 y_2}{m_1 + m_2}$$
(3)

In this equation, y_{cm} is the position of the center of mass in centimeters, m_1 and m_2 are the masses of the bottom cylinder and top cylinder, respectively, and y_1 and y_2 are the positions of the center of mass of the bottom cylinder and top cylinder, respectively. For a simple pendulum at small angles, equation 4 approximates the period of the pendulum.

$$T_o = 2\pi\sqrt{\frac{L}{g}} \tag{4}$$

In equation 4, g is the gravitational constant, which is approximately $9.81\frac{m}{s^2}$ ($981\frac{cm}{s^2}$). However, this equation has significant error at greater angles, which are certainly possible in this scenario, so an extension of this equation (equation 5) as derived in [41, 45] is used to approximate TTRE. Note that the equation is divided by two due to the combination of arresting, as well as time to offset the system due to initial torque. Since only a quarter of a period occurs given the assumption that the ring is arrested the first time it passes through its intended equilibrium point, the equation is divided by four. It is then multiplied by two because TTRE must also account for the time it took for the ring to be offset to the position where net torque is 0 based on initial UE rotation. A worst case estimation is that it will take the exact same amount of time it takes for the system to do $\frac{1}{4}$ of a period so TTRE is approximately equal to half of a period of the pendulum.

$$TTRE = \frac{T_o}{2}(\frac{sin(\theta)}{\theta})^{-\frac{3}{8}} \tag{5}$$

In equation 5, θ is the maximum angle that the ring reaches, relative to where it began at rest. While equation 5 is a much better approximation than equation 4, it still has some error and table 3.1 gives the inaccuracies of the two equations.

Percent Error				
Equation #	$\theta < 20°$	$20° \leq \theta < 40°$	$40° \leq \theta < 70°$	$70° \leq \theta < 90°$
Equation 4	$< 1\%$	$< 3\%$	$< 10\%$	$> 10\%$
Equation 5	$< 0.1\%$	$< 0.1\%$	$< 0.1\%$	$< 0.4\%$

Table 3.1: Percent Error of Simple Pendulum Small Angle Oscillation Equation [54] vs Approximation Given by eqn. 6 [41, 45].

In order to calculate the TTRE for the case given by figure 3.8, some constants must be assigned. For this calculation, it will be assumed that $m_1 = 0.25kg$ and $m_2 = 1.00kg$ and that the PD and IR emitter are massless. The cylinders are assumed to be perfect right cylinders, so the center of mass of each of them is their centroid. The y-axis is assigned to the centroid of the top cylinder, so that position $y_1 = 0$. Each cylinder is assigned a height of 2 cm, so the position of the bottom cylinder is $y_2 = -2$, or 2 as long as the direction is kept in mind. As previously stated, $\theta = 45°$ and $g = 981\frac{cm}{s^2}$. Using these numbers, it is determined that y_{cm}, the center of mass of the point mass described by the combination of the two cylinders, is at $y = 1.6cm$, which is 1.6 cm below the line formed by connecting the two gimbals, or the pivot point. This value equals L and is subsequently applied to equation 5. From this it is determined that the TTRE for a UE rotation of 45° is 0.1320 seconds $\pm$ 0.00013 seconds. Figure 3.9 plots the TTRE with the previously stated assumptions based on different θ's ranging from 0°-179°.
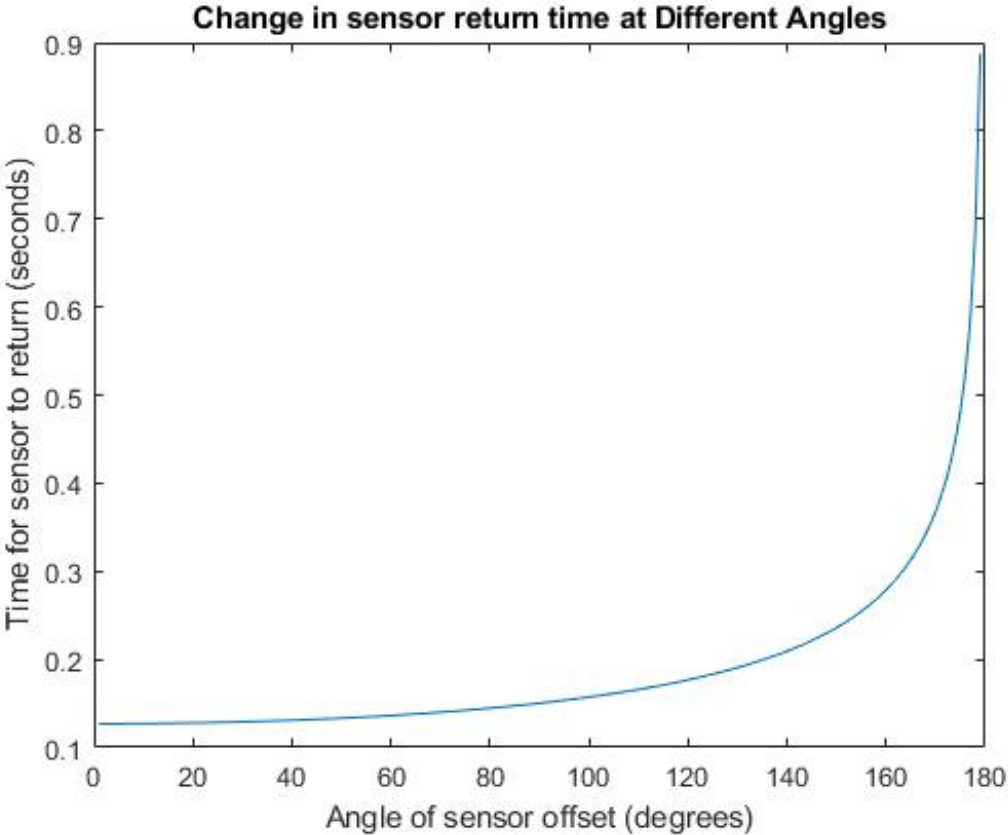

Figure 3.9: TTRE for Different θ's in Range 0°-179°.

Figure 3.9 shows that TTRE is quite small for most rotations, and as expressed

previously, assuming the coefficient of static friction is never broken and the angle of ring rotation equals the angle of UE rotation are worst case assumptions, TTRE would likely be better for most cases. It is worth noting that $\theta = 180°$ was omitted from the plot, as TTRE $= \infty$ for $\theta = 180°$. This is one of the two cases mentioned previously where this system falls short. For θ to equal $180°$, however, the user would have to rotate their UE in such a way that the bottom cylinder would perfectly balance on top of the top cylinder upside down. While this is theoretically possible, it is essentially impossible in practice and is not a reasonable concern. The other case where the RI system would fail to be effective is if the UE was rotated about the x-axis by $90°$. This would position the system perfectly under the device, so it would have little to no visibility, depending on the position of the AP. This device position looks as shown in figure 3.10.

Figure 3.10: Potential RI Failure Case of $90°$ Rotation About the x-axis.

While unlikely, it is possible that the user would want to use their UE while doing a headstand or handstand, but in cases like this where received signal strength indicator (RSSI) is too low for too long based on TTRE, a simple VHO would take place as usual [52]. In most cases though, rotations would likely be between $0°$-$90°$.

The TTRE for these cases is given by figure 3.11.
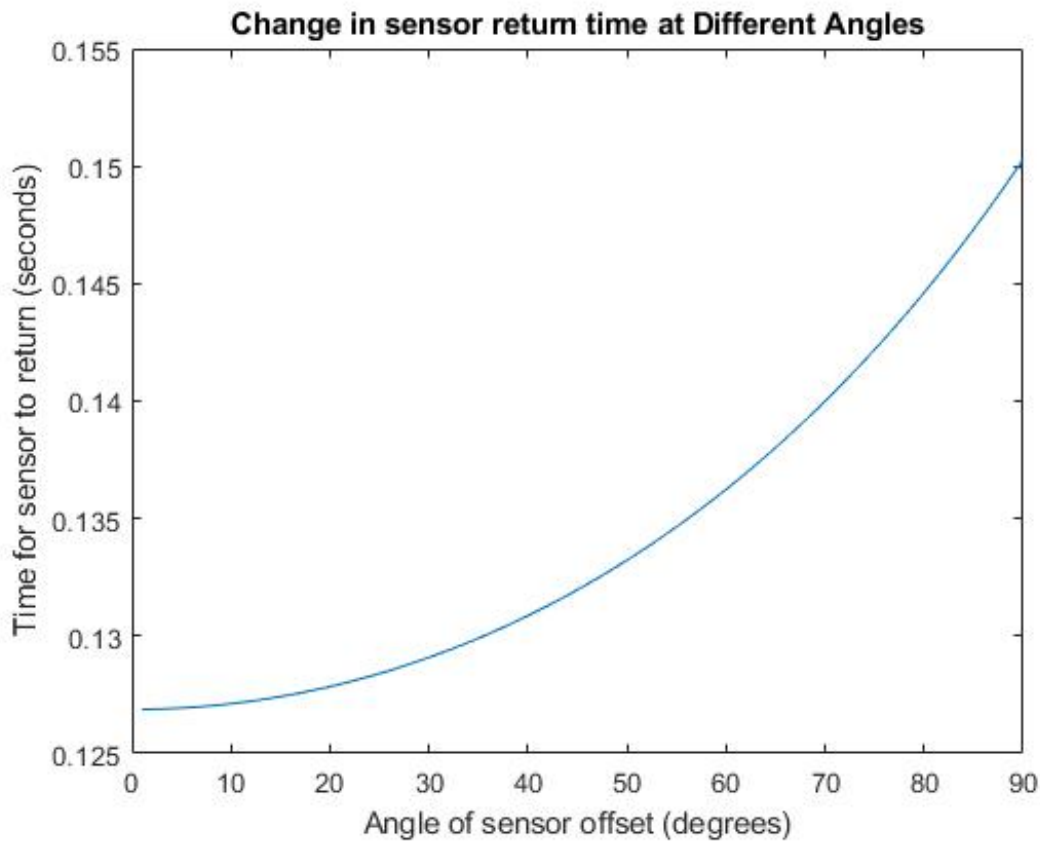
Figure 3.11: TTRE for Different θ's in Range 0°-90°.

While many different algorithms can determine if a VHO or HHO should occur, this decision is often made based on the amount of time with poor RSSI, throughput, BER, or SNR compared to the metrics that would be available should a handover occur [4, 52, 62, 66, 67, 68]. Since most handover algorithms are dependent on the performance of other available LiFi/WiFi APs, it cannot be said with absolute certainty that the TTREs shown in figure 3.11 will be small enough that handovers will not be necessary without experimentally testing the RI design on a hybrid network. This is an important area of future research, as it would empirically prove the effectiveness of the proposed design. However, the papers cited above typically assume total blockage of the PD, leading to a handover, and the proposed design would almost never have total blockage (except for the two unlikely edge cases discussed previously). Furthermore, all of the TTREs for angles 0°-∼ 150° are less than ∼ 0.2 seconds, so with this RI system, VHOs would likely not be required. In cases where the angle is greater than ∼ 165° a VHO would take place as usual and the

user would be serviced by WiFi.

3.5   Ring Arresting (Part 3 of Physics Problem)

It was stated previously that the RI system is assumed to arrest the first time it passes through its new equilibrium point after a rotation, or after $\frac{1}{4}$ of a period. This means arresting the ring is assumed to be effective enough to stop any significant oscillations due to the "pendulum problem" part of the scenario. There are many ways this can be done and it is primarily an engineering design problem rather than a physics or computer science problem, so while some options will be discussed, the specific design choice will be left to future work.

One method that could prevent oscillations is magnetic braking. Described by Faraday's Law of electromagnetic induction, when metal is placed in a time-dependent magnetic field, an electrical field is induced and circulating eddy currents are generated, which dissipate the energy in the metal. Furthermore, if a metal is moved through a stationary magnetic field these eddy currents will induce a magnetic drag force, slowing down the motion of the metal based on the Lorentz force law [64]. If such an environment was created around the metal rings in the proposed design, the same effect would occur to slow oscillations. This would also slow the offset due to initial torque, as well as the return to the intended new equilibrium point. So, the system in general would be more resistant to changes if magnetic braking is used at all times. However, an important consideration in this method is that the presence of magnetic fields could impact UE functionality. The flow of electrons is influenced by magnetic fields, as are other internal magnetic sensors in the UE. This design would also require that the RI system be surrounded by these magnets on at least two sides. While transparent magnets do exist, path blockage or alterations in light propagation are a concern.

Magnetic attraction is another method that could slow oscillations. Envision a transparent spherical casing with a thin shell, inside of which is a magnet that surrounds the RI system. This magnet is free to move throughout the shell as the device is rotated, but its motion is slowed by friction between it and the inner/outer

layers of the shell. Furthermore, the lower cylinder attached to the pole of the inner ring is magnetic with the opposite polarity as the magnet inside the shell. This would cause an attractive force between them. Additionally, due to gravity, the magnet would seek the lowest possible point, bringing the lower cylinder with it due to their attractive force. This would also likely slow down the offset due to initial torque, and would slow or stop oscillations due to the magnetic attraction, depending on the strength of the magnets. The design would be vulnerable to wear over time due to friction between the magnet and the shell casing. Additionally, a possible concern is one of the fail cases of the RI system previously mentioned, where if the magnet is perfectly balanced on top of the sphere, the force of gravity would not pull it to the lowest point and therefore it would not slow or stop any oscillations. However, this is unlikely and would be resolved with any further applied torque on the UE.

Another option is liquid braking. Liquids have the property of conforming to the shape of their container, and are subject to the force of gravity. If one were to hold a bottle of water with two fingers at the midpoint of its height on opposite ends, rotate it to an angle and release, the water would fill the lowest point in the bottle, thus returning it to its original position. This example is analogous to the idea of braking with a liquid. If the bottom cylinder is heavier than the top and they are hollow, filled partially with water, when the ring is offset due to torque applied to the UE, the weight of the cylinder and the water would cause the system to seek the intended position where the PD/IR emitter are parallel to the AP plane. Furthermore, because the water always seeks the lowest point in the cylinder, its oscillations will be slowed due to the weight of the water pushing against the side of the cylinder opposite the direction of rotation.

Lastly, friction braking is a possible solution to prevent oscillations. Without using any sensors or intelligent system, this can be done by increasing the coefficient of friction on the gimbals at all times. However, while this will slow oscillations faster than a system with less friction, it will also cause the ring to be further offset. Additionally, this method would wear at the gimbals over time due to friction and become less effective, necessitating periodic replacement. On the other hand,

magnetic and liquid braking only release energy in the form of heat, which is negligible.

The water braking idea would be feasible from a purely mechanical standpoint, which is beneficial in minimizing complexity and logic required to make the system functional. However, magnetic braking, magnetic attraction, and friction braking could all make use of the UE's other sensors to more intelligently perform their function and brake more efficiently. UEs have a built in electrical gyroscope, which provides feedback to the phone's CPU. This sensor allows the CPU to determine rotational motion or changes in orientation, therefore making it aware of these external torques applied to the UE. So, after a rotation of the UE, the CPU could determine how far it was rotated or the direction of the ground and communicate with the braking system to apply one of these three techniques exactly at the intended equilibrium point in its oscillation, thus stopping it abruptly in the ideal position where the PD/IR emitter will be parallel to the LAP plane again. While using this "smart" braking method requires more complexity, it would likely yield better results and be closer to the assumption in this thesis of stopping any significant oscillations at $\frac{1}{4}$ of the period of the pendulum the first pass.

Lastly, with advances in ML and materials science, more versatile PD receivers could be configured to create a smart PD/IR positioning system or an absorbent mesh material receiver. These concepts are further explained in appendix A1.1 and A1.2, respectively.

4 | Predicting User Movement for Optimal Handovers

In a hybrid WiFi/LiFi network, VHOs and HHOs are required depending on the availability of those networks. Currently, most papers handle these handovers in a reactive manner, meaning they do not perform a handover until some metric is degraded beyond a tolerance, whether it be QoS, RSSI, data rate, etc. However, it is has been proven in previous works [14, 60] that the movement of humans is predictable and can be learned using different forms of ML. Additionally, algorithms that do not require ML could be used to track "hot spots" in a room and identify common patterns of humans interaction in certain spaces.

In this chapter it will be proven that by predicting human motion in a room, handovers can be performed in a proactive manner and QoS will be improved. Each component of the requirements to implement such a system will be explained individually and proven, then the entire system will be tied together. To implement such a system, it is required that: (1) data on user position and orientation is available to serve as input to the algorithm (2) human movement can be predicted accurately (3) performing proactive handovers will improve QoS.

4.1 Availability of Relevant Data

In order to make any prediction on future UE position and/or orientation, a model must be trained and input will be required to feed into this model to make predictions at deployment time. As a result, it is essential that data on UE position and orientation can be collected with high accuracy. The next few paragraphs describe different forms of input data and ways it can be collected reliably.

Assuming that the UE is connected to some LAP in a particular room, using the

signal-to-noise ratio (SNR) as input to a deep learning (DL) model can be highly effective in determining current position and orientation. In [7], $x, y, z, \alpha, \beta, \gamma$ were determined by using SNR as input to a convolutional neural network (CNN) and multi-layer perceptron (MLP). During an offline phase, a dataset was collected including received SNR at different APs for the possible positions and orientations of UE. A CNN was trained on this data and during an online phase, its predictions were tested against real UE position and orientation. Ultimately, it was found that with a CNN, user position and orientation could be determined in an average of only 18 ms with high accuracy (see table 4.1)

Metric	Avg Error (LOS)	Avg Error (LOS + Non LOS)	Precision (LOS)	Precision Error (LOS + Non LOS)
Position (cm)	16.49	10.53	29.8	17.15
Yaw α (deg)	11.9	9.07	16.9	12.5
Pitch β and Roll γ (deg)	1.42	0.96	3.19	2.135

Table 4.1: Performance of CNN in Estimating UE Indoor Position and Orientation [7].

The orientation of UE can be determined independently as well, meaning that no handshake between the device and AP is needed. In [11], UE orientation was able to accurately and quickly be determined using sensors that are inherent to the device. Based on a combination of measurements from the phone's 3-axis magnetic field sensor, which outputs roll, pitch, and yaw, the phone's 3-axis gyroscope, which determines angular rotations, and the phone's KR3DM sensor, which measures accelerations with respect to the phone, [11] was able to mathematically correct for errors due to magnetic fields and degradation over time to determine the phone's α, β, γ with a 6% maximum error.

Several other works such as [9, 37, 49] have studied IPSs and shown that its quite simple to determine user coordinates in a room with high accuracy.

Both of the works evaluated show that data on the UE's position and orientation are readily available, accurate, and could be used as input to an algorithm that is predictive of future human movements. In section 4.2, more works will be evaluated that have used similar data collected using laser ranging sensors to make these

predictions.

4.2   Predicting Human Movement and Tendencies

After collecting data on current UE positions and orientations, a dataset can be compiled, which can be used to test the hypothesis of humans being predictable in their indoor moving tendencies. With this prior knowledge, forms of probabilistic ML and other prediction algorithms can be used to create motion models and will be shown to predict motion with accuracy.

Many papers that sought to predict human motion were in the context of intelligent robotics and focused on the importance of learning human behavior to improve human-robot interactions. While many would surmise that their movements and decisions are unique and unpredictable, humans make decisions based on intent and within an indoor environment there are certain "hot spots" that are frequented. While at any point in time one could be walking and decide to be erratic in their movements or change their intended destination, similar paths and tendencies are the norm. Figure 4.1 is a visualization of real recorded data of human motion in an office that demonstrates this. As evident in the figure, there are common paths and several clusters of blue that represent "hot spots."
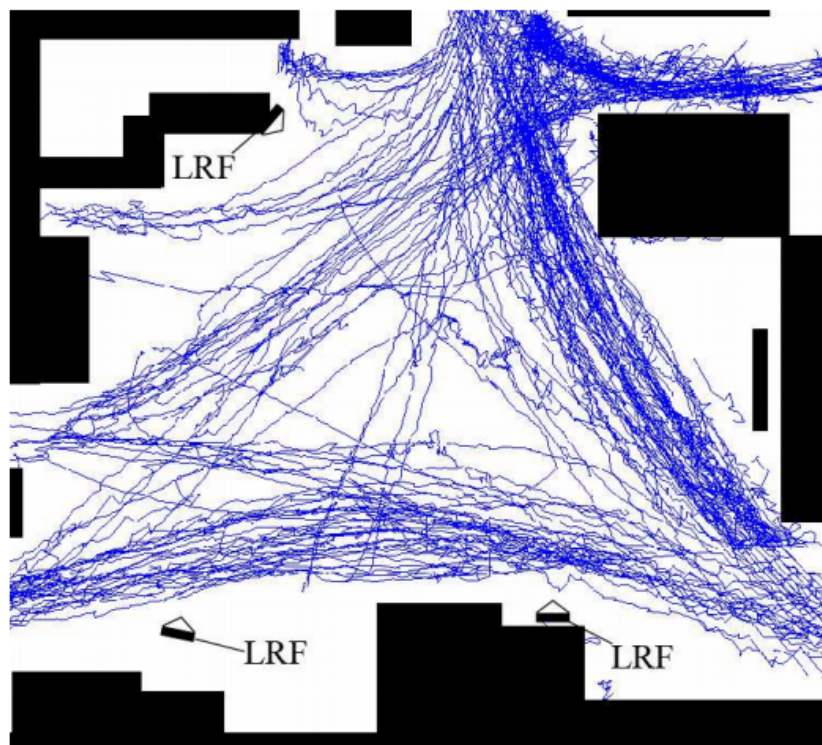
Figure 4.1: Visualization of Real Recorded Human Motion in an Office Setting [60].

Referencing figure 4.1, it is clear that certain paths are frequently traveled and by tracking prior data of motion, human tendencies can be learned, even without ML. By tracking how long individuals spend in each particular "hot spot" and generalizing frequented paths, at each moment in time at runtime, a probability distribution can be determined across all possible movements the person could take. For example, say an individual was in hot spot A and has stood up and takes one step in a direction. Based on the coordinates thus far, there is a 75% chance that they will move along path A and a 25% chance they follow path B. As the individual takes more steps, the probability that they are on one path A will either increase or decrease depending on whether or not they continue following the generalized path A. Additionally, it is critical to allow some tolerance of error, as it is clear from figure 4.1 that even if the destination is the same between two paths, sometimes humans follows slightly different paths. Furthermore, it is critical to keep in mind that the purpose of this tracking is ultimately to better perform handovers and improve QoS. In a common indoor scenario, there likely will not be many LAPs, so perfect tracking of small nuanced differences in user path are unimportant, as this would not affect whether they are connected to one AP or another.

Further down the same line of making probabilistic predictions of motion, the priors generated by tracking motion over time can be leveraged to train a ML model to accurately predict motion as well. [14] focused on forecasting movement when sensor visibility of a human is lost in a robotics context. By using a particle filter, [14] developed a complex motion model that operated under the assumption that "people's movements through a space can be represented at a high level as progress towards one of a finite set of goals." Against a simple but common Brownian motion predictor, which makes a naive assumption that at each step a person's motion is independent of any priors, this algorithm performed quite well and figure 4.2 shows a comparison of the normalization constants of the two.
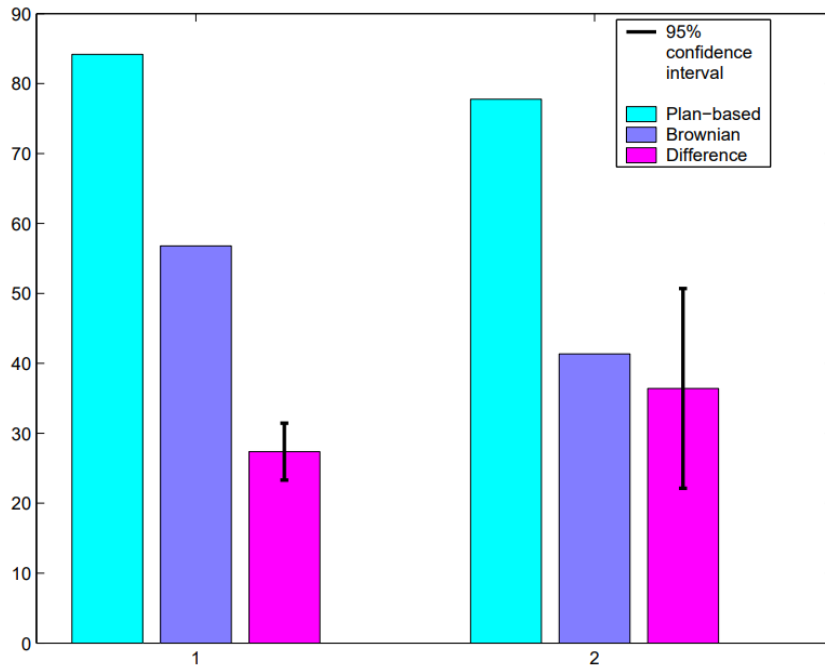
Figure 4.2: Comparison of Normalization Constants for Plan-Based Predictor (motion model) vs Brownian Motion Predictor [14].

[60] followed a similar approach, determining a probability distribution over possible movements under the assumption that navigational intent dictates motion. Based on priors and current predicted intended goal and velocity, [60] was able to accurately predict motion (see figure 4.3). While the accuracy appears low as time increases, it is actually quite good because the prediction is made for the entire duration at $t = 0$ seconds and in a real implementation, the prediction would be made at each time step so the accuracy would be more similar to the leftmost parts of the graph.
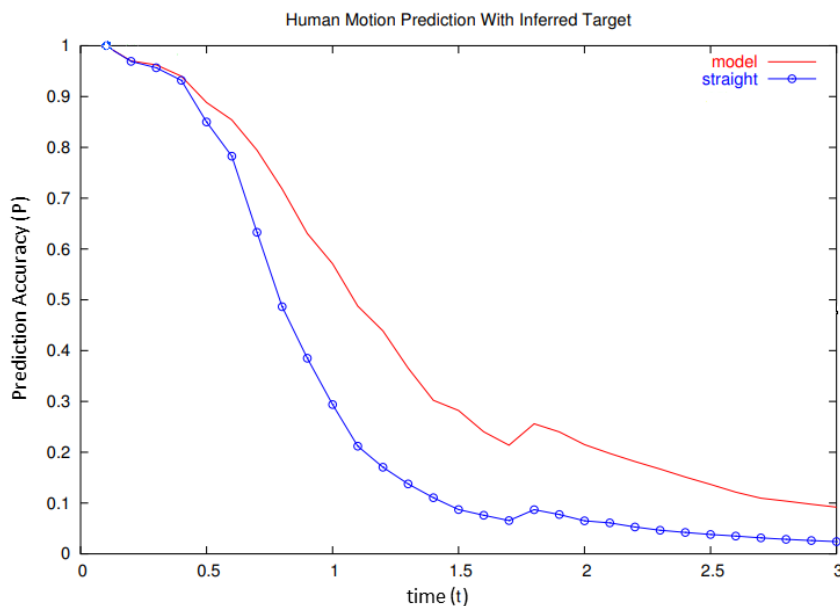
Figure 4.3: Comparison of Motion Prediction Accuracy for Probabilistic ML Approach vs SMM [60].

To further improve accuracy, this paper also accounted for the human's FOV under the assumption that people look in the direction they intend to move. In figure 4.4, this concept is showcased as the blue 'x' is the person's current position and the colored areas extending from it represent most likely directions of motion given the person's FOV.
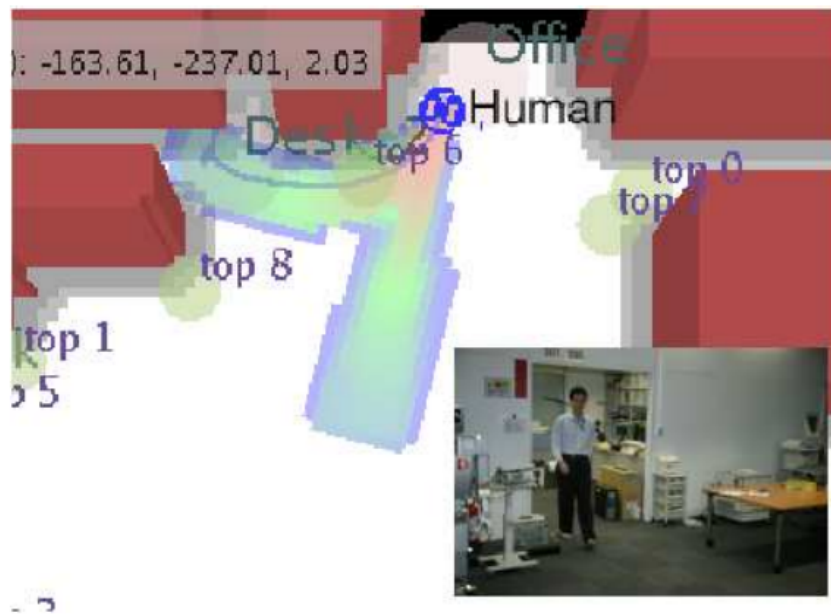
Figure 4.4: Visualization of Human FOV Influence on Weighting of Prediction [60].

A beneficial area of future research is to attempt to predict human movement using RL. With a reward function focusing on having accurately predicted motion in a discretized space, it is believed that "hot spots" and frequented paths will be discovered. Furthermore, an on-policy algorithm is proposed so that Q-values will be updated based on both the next state and the current policy's action, given that the policy likely should depend directly on the action of the human at the current state. This will also allow it to be deployed initially without any prior training and improve significantly as more data is gathered.

4.3 Impact of Accurate Movement Prediction on QoS

It has been proven that (1) data on UE position and orientation can be determined accurately and (2) the future movements of humans can be predicted using this data.

Lastly, it is critical to prove that performing effective handovers will improve QoS, which subsequently demonstrates that motion tracking to better perform "make-before-break" handovers is beneficial.

[65] studied handover skipping for HHOs. This paper focused on scenarios where a user starts in AP-A area of operation (the area where RSSI is currently greatest) and is moving in a straight line and passes through AP-B area of operation briefly and continues into AP-C. Figure 4.5 shows a visualization of this scenario.
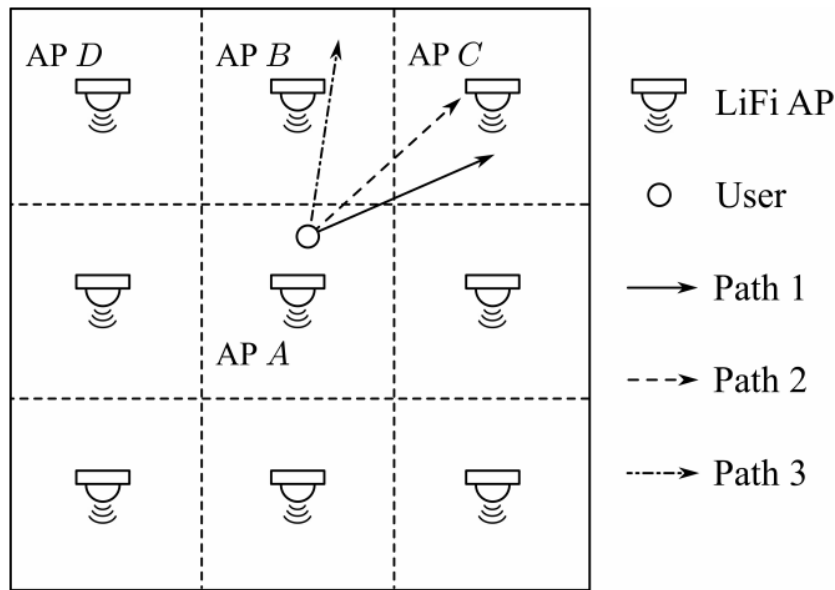
Figure 4.5: Visualization of Possible Paths of User; Handover Skipping is Useful for Path 2 [65].

Rather than transferring them to AP-B, then to AP-C, which is an example of the "ping pong effect," AP-B can be skipped and the user will directly transition to AP-C. With this algorithm, [65] found that, compared to standard handover schemes, which reactively perform handovers when metrics like RSSI degrade beyond a tolerance, this algorithm reduced handover rates by 29% and improved throughput by 66%.

It is clear from [65] that performing handovers more intelligently and proactively can significantly improve QoS and system performance as a whole. However, this paper assumed the SMM, which expects a human to move in a straight line directly from point A to B. Referencing figure 4.3 from [60], it was shown that through a probabilistic ML approach, a more accurate prediction of human movement can be made. Furthermore, if a more accurate model for user motion is created, then it is

expected that the results of [65] will further improve because in reality humans do not follow straight paths, especially in the presence of obstacles in a room. This more accurate model would theoretically perform better in handover skipping and would allow for non-linear skips as well.

4.4   Discussion

In this chapter, it has been shown that predicting human motion is feasible with the information and algorithms available, as well as beneficial from a QoS standpoint. The dataset and model would be stored in the CU, which performs the predictive algorithm and handover skipping algorithm. It is believed that different people have somewhat different tendencies in the same space, and it is possible to create a more personalized predictor. When an individual walks into a room for the first time, some unique identifier can be stored for them and a dataset can be compiled that learns exclusively the tendencies of that individual. Then, whenever they enter the room another time, their identifier is sent to the CU, which applies the model specific to that individual. While this may be more nuanced and accurate, it will require more computational complexity, storage space, and has privacy concerns. Instead, it is proposed that a more generalized model is created for any individual in that space.

It is important to note that the predictive algorithms explained in section 4.2 only predicts future coordinates. To the knowledge of the author, no prior research has been done to predict UE rotations, which is a critical area for future work. It is believed that UE orientations are also predictable, as people orient themselves in particular manners depending on their environment (e.g person laying on their back in bed or sitting up straight at their desk), but this hypothesis must be explored further.

While no papers have been found that perform "smart handovers" by predicting future user motion based on priors, papers have used RL to improve load balancing. [3] explored optimizing AP assignment through RL with a reward function focused on maximizing long-term system throughput while ensuring user fairness. Similarly,

[61] used a specific type of RL called multi-armed bandit to perform optimal AP assignment. Both of these papers published successful results, improving long-term QoS, and it would be beneficial to use the techniques they describe in conjunction with the human motion prediction concept explained in this chapter for even better performance.

Ultimately, this chapter works off of the assumption that data can be collected and processed at a rate fast enough and that the algorithm is accurate enough that performing proactive handovers improves QoS. It has been shown in other works [39] that humans signal movement intent through many components of their body. With advances in computer vision, it is quite possible to leverage ML algorithms in this field to further improve prediction accuracy through things like joint and limb identification and tracking (the movement of these were shown to be key in identifying motion intent [39]). In this chapter it was shown that tracking and predicting human motion in an indoor environment could be very beneficial in performing optimized handovers, but it has yet to be empirically proven and it is essential that future works tie together the concepts proven individually in sections 4.1, 4.2, and 4.3 to show that the idea as a whole has merit.

5 | LiFi/WiFi Bandwidth Aggregation at the Physical Layer

5.1 Introduction

As explained thus far, any phenomena that can vary in nature and can be received by some sensor can be used as a medium to transmit data, even something as simple as a piano. In the piano example, a 2-FSK system was described where one key (or frequency) represents a 0 and another key represents a 1. As more keys on the piano are used, more bits can be sent simultaneously. In fact, the precise number of bits that can be represented equals $\lfloor log_2(k) \rfloor$ where k is the number of keys involved in the encoding scheme. This can be scaled up, only limited by the number of different modulations possible and the sensitivity of the sensor, or its ability to distinguish one key from another. This scaling up process will be referred to as increasing the number of levels.

As the number of levels are increased, more bits can be sent in the same time period than another scheme with less levels. The data rate is subsequently increased as well, which is a crucial metric in computer networks and significantly impacts user QoS.

Naturally, the goal of increasing the number of levels translates directly to LiFi and WiFi, where finding ways to increase the number of levels will increase data rates and therefore is an important area of research. To represent different levels to send bits, state-of-the-art LiFi uses MM as discussed in chapter 1 and WiFi systems typically use quadrature amplitude modulation (QAM), which is essentially a combination of ASK and phase shift keying (PSK).

Previous works have researched leveraging multiple forms of networks or connections when both are available to increase data rate and improve user QoS through a process called bandwidth aggregation (BWA). Most of the research in this realm has focused on aggregating signals from WiFi and broadband cellular. BWA can be done at several levels of the Transmission Control Protocol/Internet Protocol (TCP/IP) stack and to the knowledge of the author, prior research has explored BWA at the data link layer [16, 17, 18, 19], the network layer [1, 23, 24, 29], and the transport layer [5, 25, 33, 43, 50, 70] for cellular and WiFi. For hybrid LiFi/WiFi networks, only a few works [8, 55, 71] are known to have studied BWA, all of which were implemented at the transport layer where the algorithm essentially serves different requests independently by either LiFi or WiFi, but services requests simultaneously. However, no prior research has been found that looked into doing BWA at the physical layer, combining the modulations received through different mediums (radio frequencies and light) into one stream of bits. This concept, termed "bandwidth aggregation at the physical layer," (BWAPL) is the focus of chapter 5.

5.2   Assumptions and Requirements

In order to properly explain BWAPL, several assumptions must be made and requirements must be met. Firstly, it is assumed that all other layers of the TCP/IP stack operate as usual. No protocols are modified and no changes are made to existing state-of-the art operations of the other four layers of the model. BWAPL focuses exclusively on bits to signal at the transmitter and signal to bits at the receiver. Additionally, it is assumed that for BWAPL to work, both LiFi and WiFi must be available to the UE. This means that the position and orientation of the UE must be one such that the PD is visible and the RF signal is strong enough. If this is not the case, then BWA is not the right choice to transmit/receive data and the UE will be serviced as usual either through LiFi or WiFi exclusively depending on which signal is not available.

Prior to applying BWA, both sender and receiver must be aware that BWA is being used so the transmitter and receiver know to emit and detect both types of signal,

respectively. As previously mentioned in chapter 3, it is fairly easy to quickly calculate the position and orientation of UE [11, 26, 49, 61] and whether or not LiFi/WiFi will be available. Based on this determination, the UE's CPU can determine that it is in a pose where both LiFi and WiFi can be received simultaneously. When data is requested by the UE, it will begin by sending an uplink request for BWA via IR, which will be received by the CU. A response will be given on downlink via LiFi confirming that the UE will be serviced by a BWA composition of signals, or on WiFi declining the request. After the IR uplink request for BWA, the UE will be sensing for a LiFi signal and a WiFi signal so it can receive the verdict of its request. After the request is confirmed, the transmitter will service the request via the BWA signals and the receiver will continue to listen over both mediums. This handshake is crucial so the transmitter knows to encode the intended bits in two signals and the receiver knows to decode both signals for that particular stream of packets. A simple encoding scheme will be discussed in section 5.4 as an example to clarify this concept.

Lastly, it is critical that synchronization between LiFi/WiFi is prioritized, since the bit stream for a particular grouping of signals depends on both signals received. There are many ways to synchronize the two, and this will largely depend on the baud rates of the mediums. However, for simplicity, it will be assumed that LiFi and WiFi either have the same baud rate or the faster of the two will be slowed to match that of the slower one, so they have the same symbol rate. Other possibilities for mismatched baud rates will be discussed in section 5.6.

5.3   Bandwidth Aggregation at the Physical Layer

BWAPL is, to the knowledge of the author, a novel technique for increasing the number of levels in a computer network and subsequently increasing data rates. As mentioned in section 5.2, it requires that both LiFi and WiFi are available to the UE and that RF/light signals are sent simultaneously. Rather than servicing requests independently through one medium, the combination of the two signals received is another way to increase the number of levels and offer great potential to increase data rate.

The process begins with the user requesting data. The CPU of the UE then determines the device's position and orientation using methods developed in [11, 26, 49, 61]. Based on UE configuration and the availability, the CPU will determine whether or not WiFi and/or LiFi are available. If one of the two is not available, the device will send its uplink request via IR or WiFi and be serviced as usual in a hybrid network system. However, if both LiFi and WiFi are available, meaning the PD will be visible to the LAP and a strong enough WiFi signal is available, a BWA request will be sent via IR uplink. From this time until the UE receives communication back from the AP, the UE will be detecting for signals over both LiFi and WiFi.

This request for BWA is received by the AP, and processed by the CU. If the CU is not able to serve both LiFi and WiFi, then a decline message will be sent via WiFi downlink to the device and it will be serviced as usual in a hybrid network system. If the CU deems it is able to serve over both mediums, a confirmation message will be sent via LiFi downlink and the UE will be serviced by both signals simultaneously. An encoding scheme must be standardized to translate bits to signal at the transmitter and signal to bits at the receiver. There are many options for how this can be done, and they depend on the different levels of MM and QAM available to the network. In section 5.4, a very simple encoding/decoding scheme will be presented to anchor this concept.

At some point, either LiFi or WiFi will likely become unavailable and the communications will need to revert to exclusively one or the other. Again, there are many ways to detect this and determining the best method to do so is an area for future research. However, two potential methods include detecting when the UE is no longer in a position to receive both signals or cutting off the BWA format when a certain number of signals for one medium is missed in a period of time.

In order to determine whether or not a user can be serviced through BWA to begin with, calculations are done to determine the UE position and orientation. These calculations can continue throughout the process of servicing the UE and if it is found that they are in a position where LiFi or WiFi would not be available, the UE can revert to typical hybrid network service. However, this idea is vulnerable to what is

known as the "ping pong effect" where users bounce between two forms of networks due to oversensitivity. As a result, it would be important to have some delay period where a network would have to be unavailable for a certain number of steps or period of time before reverting. This would reduce the sensitivity compared to a system that switches immediately between the BWA LiFi/WiFi and typical hybrid network service when a signal is not received. When hybrid networks were first developed and the idea formed to switch between LiFi and WiFi when one loses signal, the phenomena of the "ping pong effect" was discovered and many papers focused exclusively on solving this problem. If the community adopts the idea of BWAPL, this will surely be a challenging problem to solve and an important area for future research, although past research on hybrid LiFi/WiFi network handovers would be a good starting point. Another concern, although minor, is that it is computationally expensive to calculate the UE position and orientation every time a signal is received.

The other idea for detecting if BWA should revert to usual hybrid network operations is much less complex. Instead of calculating the pose of the UE, it is simply detected whether or not both signals were received at a particular time step. If one of the signals is not received, then the system can revert. Again this idea is sensitive to the "ping pong effect" and would require research into determining when the appropriate time is to switch between BWA and exclusively LiFi or WiFi.

Both of the methods for reverting from BWA involved a decision made either at the time of signal receipt or after it. With advances in ML, in particular RL, an interesting area of future research is to predict in advance how UE will translate or rotate and whether or not both light and radio signals will be able to be received.

Regardless of the method to decide whether or not to revert from BWA, at some point this decision will be made by the UE's CPU or the CU. If the UE's CPU recognizes that both LiFi and WiFi are not available, it will send a request via IR uplink to return to purely LiFi or WiFi, specifying which one to transition to. The AP will receive this communication and notify the CU, which will send a downlink confirmation of the agreement via the available medium. If the CU decides that it cannot service over

both LiFi and WiFi, it will only send over the available medium. Eventually, per the previous few paragraphs, the UE CPU will recognize that it is not receiving one of the necessary signals and it will then send the request to transition to pure LiFi or WiFi.

Another significant concern of BWAPL is synchronization. LiFi and WiFi often have different baud rates, or number of signals modulated per second. In order to combine both signals into one bit stream, they must be synchronized in a manner that can be standardized. For example, if the baud rate of LiFi is twice that of WiFi, an encoding scheme could be used to decode at the rate of WiFi, but the mapping of signals to bits would involve two LiFi signals and one WiFi signal. While the baud rate of one medium could be slowed to match that of the other, this would not make the best use of the maximum possible data rate, as more levels can be achieved through the receipt of three signals (two LiFi, one WiFi) than two. If the baud rate of one signal does not divide evenly by the baud rate of the other, the problem becomes a bit more difficult, as 1.5 signals are received over one medium to one signal over the other, for example. However, it is possible to develop a modulation scheme that accounts for this and it would still be beneficial to increasing data rates. The primary concern with synchronization is simply consistency in the baud rate of each signal independently. If either is not perfectly consistent, they will become more and more offset over time until signals begin to overlap with preceding or following signals and errors occur. This issue can be solved by ensuring that LiFi and WiFi are independently synchronized to the same clock of the CU. State-of-the-art synchronization schemes such as Manchester Encoding or a non-return to zero (NRZ) variant are easy choices to do so.

5.4   Simulation Setup

In order to anchor this concept with an example BWA system, it is useful to establish a very simple simulation and state further assumptions. It is noted that all assumptions made in section 5.2 still hold. Next, it is assumed that the WiFi network operates under a basic 2-FSK scheme using the signal to bit translations shown in

table 5.1.

Frequency (Hz)	Bits
500	0
1000	1

Table 5.1: WiFi 2-FSK Signal to Bits Encoding Scheme.

Additionally, it is assumed that the LiFi network utilizes a 2-IM/ASK scheme with the mapping shown in table 5.2 where two luminous intensity values represent different bits.

Luminous Intensity (lm)	Bits
300	0
400	1

Table 5.2: LiFi 2-ASK Signal to Bits Encoding Scheme.

Furthermore, for simplicity in this simulation it is assumed that the baud rate for both LiFi and WiFi will be identical of value 1 symbol/second, although as explained in section 5.3 the two would likely be different and regardless of each medium's baud rate, an encoding scheme can still be developed using BWAPL.

With this combination of synchronized signals available from the 2-FSK WiFi and 2-IM/ASK LiFi, they can be encoded and decoded at the physical layer with simultaneous transmissions using the scheme in table 5.3.

Luminous Intensity (lm)/Frequency (Hz)	Bits
300/500	00
300/1000	01
400/500	10
400/1000	11

Table 5.3: LiFi/WiFi BWAPL Between 2-FSK and 2-IM/ASK Signal to Bits Encoding Scheme.

Table 5.3 shows that two bits can now be sent simultaneously rather than just one, thus increasing the number of levels of the network as a whole, because BWA does not require any level increase from LiFi or WiFi independently. In other words, more bits can be sent at a time while still using the exact same frequencies and luminous intensity signals.

Figure 5.1 portrays a simulation of communicating the message "I love BWA" over a combination of LiFi and WiFi using the table 5.3 encoding scheme. It shows the result of this compared to transmitting the message purely over one network or the other and it should be noted that the BWA message required half as many signals as the independent networks each did in this case.
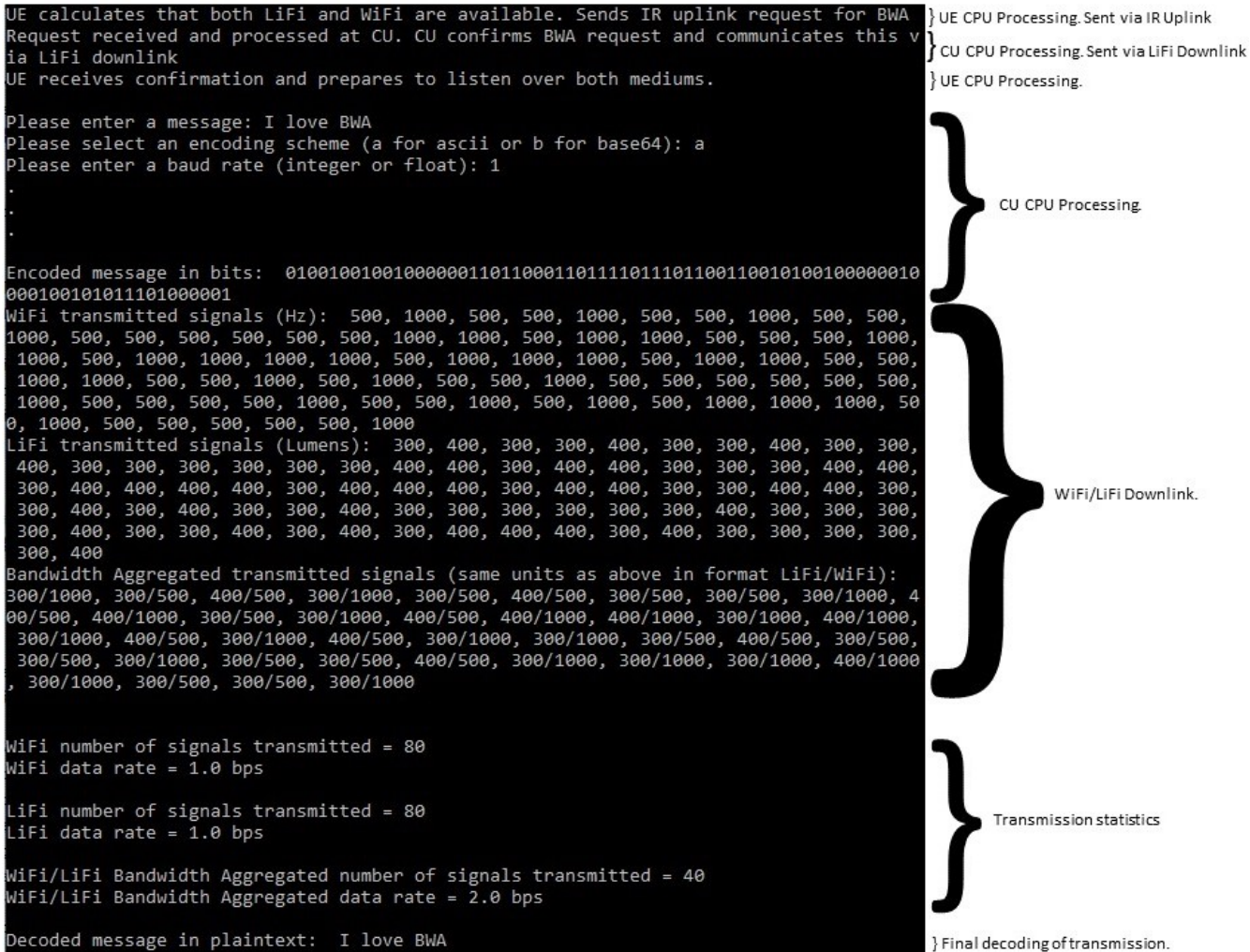
Figure 5.1: Simulation Result of Transmitting "I love BWA" over WiFi, LiFi, and BWAPL LiFi/WiFi.

In a real commercialized system, many more steps would occur prior to transmitting this message at other layers of the TCP/IP stack and the bit stream would be longer due to things like hamming bits and heades/tailers. However, for simplicity and proof-of-concept, after establishing a handshake between the transmitter and receiver, to send the message this simulation took plaintext, used either ASCII or Base64 encoding, converted to bits, and converted the bits to signals based on the encoding

schemes in tables 5.1, 5.2, and 5.3 for WiFi, LiFi, and BWA LiFi/WiFi, respectively. This transmission was received and the signals were decoded back to bits using the inverse of the mapping of the tables, then to plaintext again as shown in the final line of figure 5.1. The phase of the networking process occurring in each line of the output is shown in figure 5.1 and is labeled and grouped to the right of the step. At the end of the transmission, statistics for data rates are shown; the effectiveness of BWAPL will be quantified and analyzed in section 5.5.

5.5   Analysis of Proposed Method

In the simulation described in section 5.4, it was calculated as shown in figure 5.1 that twice the data rate was achievable for the transmission "I love BWA" with BWAPL rather than exclusively over LiFi or WiFi. However, this is just one specific example and it is crucial to generalize how effective BWAPL is compared to standard LiFi and WiFi, as well as BWA at the transport layer as shown by [8, 55, 71].

Firstly, regarding the number of bits that can be sent per clock cycle, LiFi can send $\lfloor log_2(n) \rfloor$, where n equals the number of different modulations possible in the LiFi network using some scheme such as MM. For the example in section 5.4, $n = 2$. Similarly, the number of bits that can be transmitted per cycle with WiFi is $\lfloor log_2(k) \rfloor$, where k equals the number of different modulations possible for WiFi using QAM or some other scheme. $k = 2$ for the example in section 5.4 as well. It is important to note that both of these expressions include the floor operator, which accounts for numbers of levels that cannot be equally divided into bits, or rather, are not a multiple of 2.

BWA at the transport layer offers great improvements over exclusive LiFi or WiFi, as the number of bits that can be sent at a time is equal to $\lfloor log_2(n) \rfloor + \lfloor log_2(k) \rfloor$. BWA at the transport layer essentially services multiple requests from the UE over LiFi and WiFi simultaneously, which is why the number of bits per cycle for LiFi and WiFi independently are summed. However, the servicing for a particular request is done exclusively over one of the mediums, so they require separate log and floor operators. BWAPL, on the other hand, is able to send $\lfloor log_2(n) + log_2(k) \rfloor$ bits per cycle. The

derivation for this is shown in Appendix A1.3.

It is clear that BWA at the physical or transport level offers the potential for more bits per cycle than purely LiFi or WiFi, given that their equations include an addition of terms. Comparing the bits per cycle for BWA at the transport and physical layer, the equations look similar, but the scope of the floor operator is significant at some values that are not multiples of 2. Figure 5.2 clearly shows that BWAPL offers the potential for more bits per cycle than BWA at the transport layer for many quantities of modulation possibilities for LiFi and WiFi.
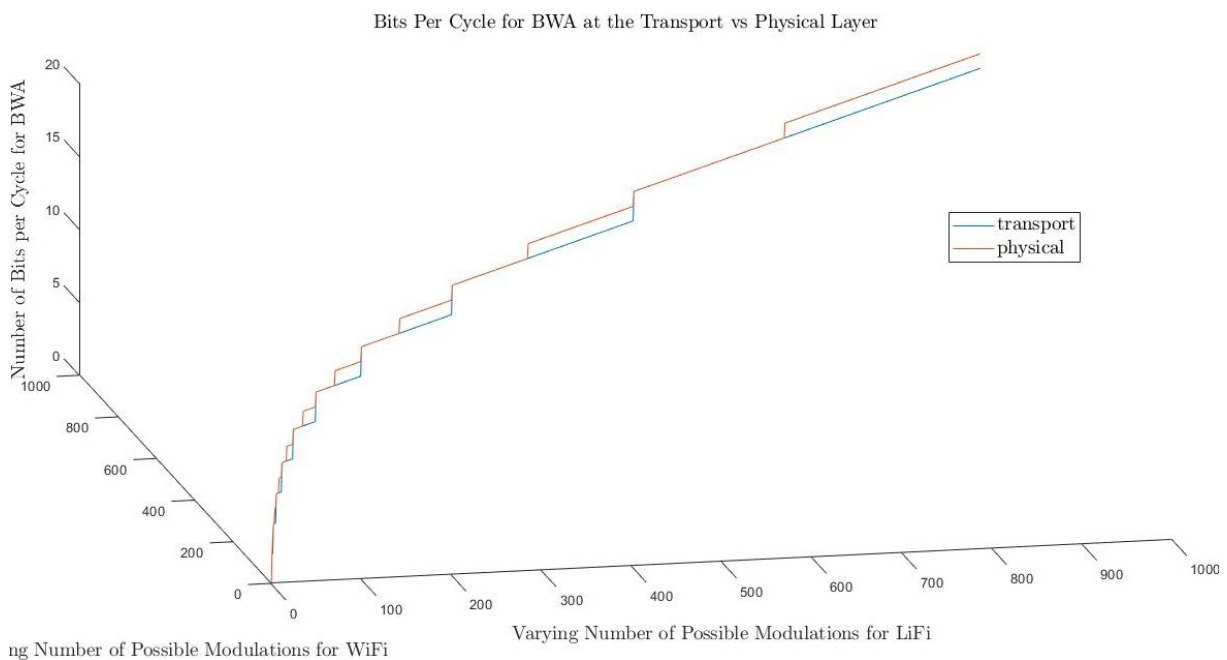

Figure 5.2: Plot Comparing BWA at the Physical vs Transport Layers.

While the advantage purely in bits per cycle for BWAPL is marginal but present, it also does not require any modification of the TCP to add extra bits or include additional flags, as the only handshake necessary occurs prior to transmission. All that is required is establishing an agreement between sender and receiver that signals are coming via both mediums simultaneously, as well as using the proper mapping for BWA. BWA at the transport layer, however, does not require synchronization between LiFi and WiFi, which could require additional overhead and complexity.

Overall, figure 5.2 illustrates the merit of BWAPL, compared to other state-of-the-art BWA techniques in the field of hybrid networking. While the math works out to

demonstrate its potential, other challenges will certainly arise when attempting to construct a physical prototype. As a result, this is the logical next step for future research, to compare the practical merit of BWAPL versus BWA at other layers of the TCP/IP stack, as well as identify and solve other issues that may arise with hardware.

5.6 Future Works and Ideas to Improve Data Rates

BWA for hybrid LiFi/WiFi networks remains largely unexplored. While a great deal of research has been done into the idea of aggregating broadband cellular and WiFi, only a few papers have been found that apply BWA to hybrid networks. In a hybrid network configuration there will inherently be two or more networks over which data can be transmitted and received. In many cases, both networks will be available at the same time and it would be a missed opportunity to always let one sit idle rather than leverage them both when possible. As proven by [8, 55, 71] and in this thesis, BWA offers significant potential for improved data rates with few drawbacks such as increase power requirements and complexity.

Additionally, to the knowledge of the author all previous works have focused on BWA for hybrid networks at the transport layer. This thesis has demonstrated the theoretical merit of BWAPL, and encourages future research to attempt to construct a prototype to explore challenging problems that may arise with hardware. While two possible algorithms were proposed for reverting back to purely LiFi or WiFi from BWA when one network becomes unavailable, more research must be done in this area to test different algorithms and these ideas must be physically tested as well.

Furthermore, there are many phenomena in this world that can be sensed and therefore offer potential for networks. Hybrid networks currently only involve WiFi and LiFi and BWA has mostly been applied to WiFi/cellular and LiFi/WiFi. However, by exploring more novel types of networks based on phenomena of the world, the potential to discover a new form of networking that will prove to be successful is increased. Additionally, by incorporating more networks into a BWA system, the

number of possible modulations increases, thus increasing the number of levels and subsequently the data rate. The number of bits per cycle would then increase to $\lfloor log_2(n) + log_2(k) + log_2(p) \rfloor$, where p is the number of possible modulations of this new theoretical form of networking.

Naturally, many phenomena would be quite impractical to form the basis of a network such as a smell-based computer network since the speed at which scents can be modulated would be slow. However, [13, 22, 56] explored an acoustic-based computer network (using FSK at frequencies outside the human range of hearing) in a terrestrial and underwater capacity which showed some merit in theory and require more research to quantify.

Regardless, it is crucial to continue to explore creative solutions in this new field. Aggregating bandwidth with alternative unconventional networks such as acoustics or smell are just a few ideas for ways that data rates can be improved. In reality, any way the signal can be varied in a manner that the sensor is able to distinguish is a way to potentially increase the number of levels and the data rate. Partially obstructing the emitted light, for example, is a way that the signal could be altered. Assuming the light is emitted with roughly a circular projection, there are an infinite number of ways that a circular projection could be partially obstructed, thus offering significant potential for increased number of bits per cycle. However, this idea is unlikely to be successful, especially from greater distances because detecting partial obstructions is unreliable and could be due to obstruction from some other object like the user's hand, not to mention the fact that it is unlikely a PD's sensitivity would be high enough to detect small obstruction modifications at all. The point being made is not necessarily about suggesting a specific idea, but rather offering a creative idea that could theoretically improve data rates. While LiFi has been studied for many years, it is critical to remain open-minded and continue to consider outside-of-the-box ideas that could prove useful in the future.

6 | Conclusion

With the spike in the number of smart devices per household and increased reliance on consuming data in the modern Information Age, it is clear that more spectrum is required for computer networks. Not only does LiFi have potential to bear this load, but it also offers several potential improvements over traditional WiFi such as better data rates and reduced radiation-related health hazards. As only a decade-old technology, brilliant developments have been made to improve LiFi and solve the challenge of path blockage to the PD. However, several problems remain to be solved before the network becomes commercially available.

The intent of this thesis was to conduct studies into three novel concepts that would make LiFi more feasible for the public. First, it was shown that path blockage issues due to rotations and translations can be ameliorated through using a rotationally invariant PD/IR emitter configuration. Additionally, the hypothesis that humans are predictable in their indoor movements based on "hot spots" and intent was proven. A smart handover concept was outlined including (1) how to access the data necessary to make predictions (2) possible algorithms that successfully perform these predictions (3) empirical proof that smart handovers improve throughput and QoS. Lastly, BWA at the physical layer through combining signals sent from LiFi and WiFi simultaneously was shown mathematically to offer better data rates than existing BWA schemes at other layers of the TCP/IP stack.

While the work in this paper demonstrated the merit of these ideas, it is important to note that each concept was described purely from a theoretical standpoint. In order to truly prove the effectiveness of these concepts, they must be validated through physical implementation, as hardware is often somewhat unpredictable and new

challenges arise with real prototypes. Furthermore, it is critical that thorough research continue in general in this field and those leading the field remain creative and open-minded, as the practical application of LiFi has the potential to impact society in a very positive and momentous way.

Bibliography

[1] IEEE Standard for Information Technology - Local and Metropolitan Area Networks - Part 3: Carrier Sense Multiple Access with Collision Detection (CSMA/CD) Access Method and Physical Layer Specifications-Aggregation of Multiple Link Segments. *IEEE Std 802.3ad-2000*, pages 1–184, 2000. doi: 10.1109/IEEESTD.2000.91610.

[2] F. Aftab. Potentials and Challenges of Light Fidelity Based Indoor Communication System. *International Journal of New Computer Architectures and their Applications*, 6, 10 2016. doi: 10.17781/P002152.

[3] R. Ahmad, M. D. Soltani, M. Safari, A. Srivastava, and A. Das. Reinforcement Learning Based Load Balancing for Hybrid LiFi WiFi Networks. *IEEE Access*, 8: 132273–132284, 2020. doi: 10.1109/ACCESS.2020.3007871.

[4] A. Ahmed, L. M. Boulahia, and D. Gaïti. Enabling Vertical Handover Decisions in Heterogeneous Wireless Networks: A State-of-the-Art and A Classification. *IEEE Communications Surveys Tutorials*, 16(2):776–811, 2014. doi: 10.1109/SURV.2013.082713.00141.

[5] I. Amezcua Valdovinos, J. A. Perez Diaz, L. J. Garcia Villalba, and T.-h. Kim. BATCP: Bandwidth-Aggregation Transmission Control Protocol. *Symmetry*, 9(8), 2017. ISSN 2073-8994. doi: 10.3390/sym9080167. URL https://www.mdpi.com/2073-8994/9/8/167.

[6] C. Archibald, Y. Zhang, and J. Liu. Human Motion Prediction for Indoor Mobile Relay Networks. In *2011 IEEE International Conference on High Performance*

Computing and Communications, pages 989–994, 2011. doi: 10.1109/HPCC.2011.145.

[7] M. A. Arfaoui, M. D. Soltani, I. Tavakkolnia, A. Ghrayeb, C. Assi, M. Safari, and H. Haas. Invoking Deep Learning for Joint Estimation of Indoor LiFi User Position and Orientation, 2020.

[8] M. Ayyash, H. Elgala, A. Khreishah, V. Jungnickel, T. Little, S. Shao, M. Rahaim, D. Schulz, J. Hilt, and R. Freund. Coexistence of WiFi and LiFi toward 5G: concepts, opportunities, and challenges. *IEEE Communications Magazine*, 54(2): 64–71, 2016. doi: 10.1109/MCOM.2016.7402263.

[9] L. Bai, F. Ciravegna, R. Bond, and M. Mulvenna. A Low Cost Indoor Positioning System Using Bluetooth Low Energy. *IEEE Access*, 8:136858–136871, 2020. doi: 10.1109/ACCESS.2020.3012342.

[10] N. Bamiedakis, K. A. Williams, R. V. Penty, and I. H. White. Chapter 11 - Integrated and Hybrid Photonics for High-Performance Interconnects. In I. P. Kaminow, T. Li, and A. E. Willner, editors, *Optical Fiber Telecommunications (Sixth Edition)*, Optics and Photonics, pages 377–418. Academic Press, Boston, sixth edition edition, 2013. doi: https://doi.org/10.1016/B978-0-12-396958-3.00011-1. URL `https://www.sciencedirect.com/science/article/pii/B9780123969583000111`.

[11] C. Barthold, K. Pathapati Subbu, and R. Dantu. Evaluation of Gyroscope-Embedded Mobile Phones. In *2011 IEEE International Conference on Systems, Man, and Cybernetics*, pages 1632–1638, 2011. doi: 10.1109/ICSMC.2011.6083905.

[12] I. T. G. "bb". IEEE P802.11 - LIGHT COMMUNICATION (LC) TASK GROUP (TG) - MEETING UPDATE, Mar 2021. URL `https://www.ieee802.org/11/Reports/tgbb_update.htm`.

[13] T. Beck, D. Fisher, M. Mattingly, and B. McDonald. Ultrasonic Data Transfer with Sound Fidelity (SoFi) Application. Bachelor's thesis, 2020.

[14] F. Broz and G. Gordon. Better Motion Prediction for People-tracking. 03 2004.

[15] P. M. Butala, J. C. Chau, and T. D. C. Little. Metameric Modulation for Diffuse Visible Light Communications with Constant Ambient Lighting. In *2012 International Workshop on Optical Wireless Communications (IWOW)*, pages 1–3, 2012. doi: 10.1109/IWOW.2012.6349697.

[16] K. Chebrolu and R. Rao. Communication Using Multiple Wireless Interfaces. In *2002 IEEE Wireless Communications and Networking Conference Record. WCNC 2002 (Cat. No.02TH8609)*, volume 1, pages 327–331 vol.1, 2002. doi: 10.1109/WCNC.2002.993516.

[17] K. Chebrolu and R. Rao. Selective Frame Discard for Interactive Video. In *2004 IEEE International Conference on Communications (IEEE Cat. No.04CH37577)*, volume 7, pages 4097–4102 Vol.7, 2004. doi: 10.1109/ICC.2004.1313320.

[18] K. Chebrolu and R. Rao. Bandwidth Aggregation for Real-Time Applications in Heterogeneous Wireless Networks. *IEEE Transactions on Mobile Computing*, 5(4): 388–403, 2006. doi: 10.1109/TMC.2006.1599407.

[19] K. Chebrolu, B. Raman, and R. Rao. A Network Layer Approach to Enable TCP over Multiple Interfaces. *Wireless Networks*, 11:637–650, 09 2005. doi: 10.1007/s11276-005-3518-5.

[20] C. Chen, M. D. Soltani, M. Safari, A. A. Purwita, X. Wu, and H. Haas. An Omnidirectional User Equipment Configuration to Support Mobility in LiFi Networks. In *2019 IEEE International Conference on Communications Workshops (ICC Workshops)*, pages 1–6, 2019. doi: 10.1109/ICCW.2019.8756852.

[21] C. Chen, D. A. Basnayaka, A. A. Purwita, X. Wu, and H. Haas. Wireless Infrared-Based LiFi Uplink Transmission With Link Blockage and Random Device Orientation. *IEEE Transactions on Communications*, 69(2):1175–1188, 2021. doi: 10.1109/TCOMM.2020.3035405.

[22] M. Chitre and W.-S. Soh. Reliable Point-to-Point Underwater Acoustic Data

Transfer: To Juggle or Not to Juggle? *IEEE Journal of Oceanic Engineering*, 40(1):
93–103, 2015. doi: 10.1109/JOE.2014.2311692.

[23] Cisco. Catalyst 3750-X and 3560-X Switch Software Configuration Guide, Release
12.2(55)SE - Configuring EtherChannels [Cisco Catalyst 3750-X Series Switches],
Sep 2018. URL `https://www.cisco.com/c/en/us/td/docs/switches/lan/`
`catalyst3750x_3560x/software/release/12-2_55_se/configuration/guide/`
`3750xscg/swethchl.html#18140`.

[24] T. Davis. Linux Bonding, Oct 2000. URL
`https://wiki.linuxfoundation.org/networking/bonding`.

[25] T. De Schepper, J. Struye, E. Zeljković, S. Latré, and J. Famaey. Software-Defined
Multipath-TCP for Smart Mobile Devices. In *2017 13th International Conference on
Network and Service Management (CNSM)*, pages 1–6, 2017. doi:
10.23919/CNSM.2017.8256043.

[26] M. Dehghani Soltani, A. A. Purwita, I. Tavakkolnia, H. Haas, and M. Safari.
Impact of Device Orientation on Error Performance of LiFi Systems. *IEEE Access*,
7:41690–41701, 2019. doi: 10.1109/ACCESS.2019.2907463.

[27] M. Dehghani Soltani, A. A. Purwita, Z. Zeng, C. Chen, H. Haas, and M. Safari.
An Orientation-Based Random Waypoint Model for User Mobility in Wireless
Networks. In *2020 IEEE International Conference on Communications Workshops
(ICC Workshops)*, pages 1–6, 2020. doi:
10.1109/ICCWorkshops49005.2020.9145333.

[28] R. De', N. Pandey, and A. Pal. Impact of Digital Surge During Covid-19
Pandemic: A Viewpoint on Research and Practice. *International Journal of
Information Management*, 55:102171, 2020. ISSN 0268-4012. doi:
https://doi.org/10.1016/j.ijinfomgt.2020.102171. URL
`https://www.sciencedirect.com/science/article/pii/S0268401220309622`.
Impact of COVID-19 Pandemic on Information Management Research and
Practice: Editorial Perspectives.

[29] E. S. Engineering, Jun 2009. URL `http://www.michaelfmcnamara.com/files/`
`NN48500-518_3.8_Switch_Cluster_SplitMlink_Trunk_SMLT_ERS_TCG.pdf`.

[30] H. Haas. Wireless Data from Every Bulb. URL `https://www.ted.com/talks/`
`harald_haas_wireless_data_from_every_light_bulb?language=en`.

[31] H. Haas, L. Yin, Y. Wang, and C. Chen. What is LiFi? *Journal of Lightwave Technology*, 34(6):1533–1544, 2016. doi: 10.1109/JLT.2015.2510021.

[32] B. Heslop. By 2030, Each Person Will Own 15 Connected Devices - Here's What That Means for Your Business and Content, Mar 2019. URL
`https://www.martechadvisor.com/articles/iot/`
`by-2030-each-person-will-own-15-connected-devices-heres-what-that-means-for-your`

[33] H.-Y. Hsieh and R. Sivakumar. A Transport Layer Approach for Achieving Aggregate Bandwidths on Multi-Homed Mobile Hosts. In *Proceedings of the 8th Annual International Conference on Mobile Computing and Networking*, MobiCom '02, page 83–94, New York, NY, USA, 2002. Association for Computing Machinery. ISBN 158113486X. doi: 10.1145/570645.570656. URL
`https://doi.org/10.1145/570645.570656`.

[34] Q. Huang, Y. Zhang, Z. Ge, and C. Lu. Refining Wi-Fi Based Indoor Localization with Li-Fi Assisted Model Calibration in Smart Buildings. 02 2016.

[35] Y. Hussein and A. Annan. Li-Fi Technology: High data transmission securely. *Journal of Physics: Conference Series*, 1228:012069, 05 2019. doi: 10.1088/1742-6596/1228/1/012069.

[36] E. Hyytia, P. Lassila, and J. Virtamo. Spatial Node Distribution of the Random Waypoint Mobility Model with Applications. *IEEE Transactions on Mobile Computing*, 5(6):680–694, 2006. doi: 10.1109/TMC.2006.86.

[37] K. Kaemarungsi and P. Krishnamurthy. Modeling of Indoor Positioning Systems Based on Location Fingerprinting. In *IEEE INFOCOM 2004*, volume 2, pages 1012–1022 vol.2, 2004. doi: 10.1109/INFCOM.2004.1356988.

[38] M. Kokholm. New study: The Decline of the Computer Continues While Newer Devices are on the Rise, Mar 2020. URL `https://www.audienceproject.com/blog/key-insights/new-study-the-decline-of-the-computer-continues-while-newer-devices-are-on-the-r`

[39] P. Kratzer, M. Toussaint, and J. Mainprice. Prediction of Human Full-Body Movements with Motion Optimization and Recurrent Neural Networks. In *2020 IEEE International Conference on Robotics and Automation (ICRA)*, pages 1792–1798, 2020. doi: 10.1109/ICRA40945.2020.9197290.

[40] C. Le Bas, S. Sahuguede, A. Julien-Vergonjanne, A. Behlouli, P. Combeau, and L. Aveneau. Impact of receiver orientation and position on Visible Light Communication link performance. In *2015 4th International Workshop on Optical Wireless Communications (IWOW)*, pages 1–5, 2015. doi: 10.1109/IWOW.2015.7342254.

[41] F. Lima and A. Palakkandy. An Accurate Formula for the Period of a Simple Pendulum Oscillating Beyond the Small-Angle Regime. *American Journal of Physics*, 74, 10 2005. doi: 10.1119/1.2215616.

[42] T. Luger. LiFi - What It Is, How It Works, What It Provides, How to Apply, and Its Future Prospects, Mar 2018. URL `https://www.led-professional.com/resources-1/articles/lifi-what-it-is-how-it-works-what-it-provides-how-to-apply-and-its-future-prospe`

[43] L. Magalhaes and R. Kravets. Transport Level Mechanisms for Bandwidth Aggregation on Mobile Hosts. In *Proceedings Ninth International Conference on Network Protocols. ICNP 2001*, pages 165–171, 2001. doi: 10.1109/ICNP.2001.992896.

[44] A. A. Matrawy, M. A. El-Shimy, M. R. M. Rizk, and Z. A. El-Sahn. Optimum Angle Diversity Receivers for Indoor Single User MIMO Visible Light Communication Systems. In *2016 Asia Communications and Photonics Conference (ACP)*, pages 1–3, 2016.

[45] M. I. Molina. Simple Linearizations of the Simple Pendulum for any Amplitude. *The Physics Teacher*, 35(8):489–490, 1997. doi: 10.1119/1.2344777. URL `https://doi.org/10.1119/1.2344777`.

[46] E. Monteiro and S. Hranilovic. Design and Implementation of Color-Shift Keying for Visible Light Communications. *Journal of Lightwave Technology*, 32(10): 2053–2060, 2014. doi: 10.1109/JLT.2014.2314358.

[47] R. Nave. URL `http://hyperphysics.phy-astr.gsu.edu/hbase/Music/pianof.html#:~:text=The%20Piano-,The%20piano%20has%2088%20keys%20which%20span%20the%20frequency%20range,to%204186%20Hz%20(C8)`.

[48] A. Nuwanpriya, S. Ho, J. A. Zhang, A. J. Grant, and L. Luo. PAM-SCFDE for Optical Wireless Communications. *Journal of Lightwave Technology*, 33(14): 2938–2949, 2015. doi: 10.1109/JLT.2015.2424456.

[49] B. Panda, H. Beria, and C. Pradhan. Deployment of Li-Fi in indoor positioning systems. *International Journal of Information Technology*, 13, 05 2020. doi: 10.1007/s41870-020-00485-x.

[50] O. Popa. Multipath TCP on mobile phones. Master's thesis, 2010.

[51] A. A. Purwita, M. Dehghani Soltani, M. Safari, and H. Haas. Impact of Terminal Orientation on Performance in LiFi Systems. In *2018 IEEE Wireless Communications and Networking Conference (WCNC)*, pages 1–6, 2018. doi: 10.1109/WCNC.2018.8377334.

[52] A. A. Purwita, M. D. Soltani, M. Safari, and H. Haas. Handover Probability of Hybrid LiFi/RF-Based Networks with Randomly-Oriented Devices. In *2018 IEEE 87th Vehicular Technology Conference (VTC Spring)*, pages 1–5, 2018. doi: 10.1109/VTCSpring.2018.8417682.

[53] A. A. Purwita, M. D. Soltani, M. Safari, and H. Haas. Terminal Orientation in OFDM-Based LiFi Systems. *IEEE Transactions on Wireless Communications*, 18(8): 4003–4016, 2019. doi: 10.1109/TWC.2019.2920132.

[54] D. Santo Pietro. Pendulums. URL
`https://www.khanacademy.org/science/high-school-physics/`
`simple-harmonic-motion/simple-pendulums/v/pendulum`.

[55] S. Shao, A. Khreishah, and M. Ayyash. Delay Analysis of Hybrid WiFi-LiFi System. *arXiv e-prints*, art. arXiv:1510.00740, Oct. 2015.

[56] A. C. Singer, J. K. Nelson, and S. S. Kozat. Signal Processing for Underwater Acoustic Communications. *IEEE Communications Magazine*, 47(1):90–96, 2009. doi: 10.1109/MCOM.2009.4752683.

[57] M. D. Soltani, A. A. Purwita, Z. Zeng, H. Haas, and M. Safari. Modeling the Random Orientation of Mobile Devices: Measurement, Analysis and LiFi Use Case. *IEEE Transactions on Communications*, 67(3):2157–2172, 2019. doi: 10.1109/TCOMM.2018.2882213.

[58] M. D. Soltani, Z. Zeng, I. Tavakkolnia, H. Haas, and M. Safari. Random Receiver Orientation Effect on Channel Gain in LiFi Systems. In *2019 IEEE Wireless Communications and Networking Conference (WCNC)*, pages 1–6, 2019. doi: 10.1109/WCNC.2019.8886097.

[59] Thales. Introducing 5G Technology and Networks (Speed, Use Cases and Rollout), Apr 2021. URL `https://www.thalesgroup.com/en/markets/` `digital-identity-and-security/mobile/inspired/5G`.

[60] S. Thompson, T. Horiuchi, and S. Kagami. A Probabilistic Model of Human Motion and Navigation Intent for Mobile Robot Path Planning. In *2009 4th International Conference on Autonomous Robots and Agents*, pages 663–668, 2009. doi: 10.1109/ICARA.2000.4803931.

[61] J. Wang, C. Jiang, H. Zhang, X. Zhang, V. C. M. Leung, and L. Hanzo. Learning-Aided Network Association for Hybrid Indoor LiFi-WiFi Systems. *IEEE Transactions on Vehicular Technology*, 67(4):3561–3574, 2018. doi: 10.1109/TVT.2017.2778345.

[62] Y. Wang, S. Videv, and H. Haas. Dynamic Load Balancing with Handover in Hybrid Li-Fi and Wi-Fi Networks. In *2014 IEEE 25th Annual International Symposium on Personal, Indoor, and Mobile Radio Communication (PIMRC)*, pages 575–579, 2014. doi: 10.1109/PIMRC.2014.7136231.

[63] Y. Wang, X. Wu, and H. Haas. Load Balancing Game With Shadowing Effect for Indoor Hybrid LiFi/RF Networks. *IEEE Transactions on Wireless Communications*, 16(4):2366–2378, 2017. doi: 10.1109/TWC.2017.2664821.

[64] H. Wiederick, N. Gauthier, D. Campbell, and P. Rochon. Magnetic braking: Simple theory and experiment. *American Journal of Physics - AMER J PHYS*, 55: 500–503, 06 1987. doi: 10.1119/1.15103.

[65] X. Wu and H. Haas. Handover Skipping for LiFi. *IEEE Access*, 7:38369–38378, 2019. doi: 10.1109/ACCESS.2019.2903409.

[66] X. Wu and H. Haas. Mobility-Aware Load Balancing for Hybrid LiFi and WiFi Networks. *IEEE/OSA Journal of Optical Communications and Networking*, 11(12): 588–597, 2019. doi: 10.1364/JOCN.11.000588.

[67] X. Wu and H. Haas. Load Balancing for Hybrid LiFi and WiFi Networks: To Tackle User Mobility and Light-Path Blockage. *IEEE Transactions on Communications*, 68(3):1675–1683, 2020. doi: 10.1109/TCOMM.2019.2962434.

[68] X. Wu, C. Chen, and H. Haas. Mobility Management for Hybrid LiFi and WiFi Networks in the Presence of Light-Path Blockage. In *2018 IEEE 88th Vehicular Technology Conference (VTC-Fall)*, pages 1–5, 2018. doi: 10.1109/VTCFall.2018.8690694.

[69] Z. Zeng, M. Dehghani Soltani, Y. Wang, X. Wu, and H. Haas. Realistic Indoor Hybrid WiFi and OFDMA-Based LiFi Networks. *IEEE Transactions on Communications*, 68(5):2978–2991, 2020. doi: 10.1109/TCOMM.2020.2974458.

[70] M. Zhang, J. Lai, A. Krishnamurthy, L. Peterson, and R. Wang. A Transport Layer Approach for Improving End-to-End Performance and Robustness Using Redundant Paths. pages 99–112, 01 2004.

[71] W. Zhang, L. Chen, X. Chen, Z. Yu, Z. Li, and W. Wang. Design and Realization of Indoor VLC-Wi-Fi Hybrid Network. *Journal of Communications and Information Networks*, 2(4):75–87, 2017. doi: 10.1007/s41650-017-0039-1.

[72] T. Zuckerman, 2007. URL `http://shakahara.com/pianopitch2.php`.

Appendix

A1 | Smart PD/IR Positioning System

Expanding further on using the device's built-in gyroscope to intelligently brake, the variables (roll, pitch, yaw, 3D position, Ω) describing the device's exact position can be known at each moment. Sections 3.4 and 3.5 focused on ensuring that the PD/IR emitter were always parallel to the LiFi AP plane, which is useful for maintaining connection to LiFi and minimizing VHOs. However, it was proven in section 3.3 that for each combination of the variables describing a user position and orientation, an ideal PD and IR angle exists. Using a smart PD/IR positioning system, these variables could be used to optimize sensor visibility at every position. Rather than using the mechanically powered three gimbal system to maintain a constant angle, three servo motors could be used to vary the angle of the PD/IR emitter based on the known variables that impact performance. This would increase the complexity of the system as compared to a purely mechanical one, but would be much more optimized and could keep the UE connected to LiFi in most cases, limited by the QoS lost during the processing time to determine the position and orientation of the device, calculate the optimal roll, pitch, and yaw angle for that pose, and move the servos to that angle.

A2 | Absorbent Material Configuration

There are more ways to detect MM than simply a single PD mounted to the top of a UE near the device's camera. While most papers primarily consider this option, as previously mentioned, some papers have explored omnidirectional receivers, and in this thesis a novel rotationally invariant PD/IR emitter configuration was proposed. Given that LiFi is still a relatively new field and is not yet commercially widespread, it is crucial to remain creative about finding solutions to the unique problems it presents. The challenge of overcoming LiFi's inherent limitation of LOS is no different.

It is proposed that future research looks into different light absorbing materials that could be used in addition to focusing on better positioning the PD. To the knowledge of the author, no previous works have explored integrating light-absorbing materials into a UE's casing to allow for omnidirectional reception of light. One such example of a material is the polymer waveguide, made from SU-8 photoresist and NOA61 optical adhesive [10]. If, for example, one's phone case had this material integrated with it, regardless of the angle or blockage of the device by a user's hands, some portion of the phone case would likely be visible, thus allowing photons to be received from theoretically any angle and position. Of course, this would not solve the problem of lack of visibility to the IR emitter for uplink, and this problem will require additional creativity and study. Additionally, to make a material like the polymer waveguide useful in receiving light, it would have to be able to communicate what it received quickly to the UE's CPU so that data can be serviced to the user. Some node on the casing would have to have contact with the device and naturally two concerns would be latency and complexity. Regardless of these issues, the overarching idea is that it is crucial for researchers in this field to remain creative

and think outside the box. While rabbit holes are useful and hybrid networks is widely believed to be a promising rabbit hole, it is critical to also take a step back sometimes and think of unique solutions.

A3 | BWA at the Physical Layer Bits per Cycle Derivation

$$x = \text{Bits per cycle}$$

$$n = \text{Number of modulations possible for LiFi}$$

$$k = \text{Number of modulations possible for WiFi}$$

$$2^x = n * k \text{ (Note: n*k must be rounded down to nearest multiple of 2)}$$

$$x * log_2(2) = \lfloor log_2(n * k) \rfloor$$

$$x = \lfloor log_2(n * k) \rfloor$$

$$x = \lfloor log_2(n) + log_2(k) \rfloor$$